© 2022. Published by The Company of Biologists Ltd | Development (2022) 149, dev200853. doi:10.1242/dev.200853

CORRECTION

Correction: FOXP4 differentially controls cold-induced beige adipocyte differentiation and thermogenesis

Fuhua Wang, Shuqin Xu, Tienan Chen, Shifeng Ling, Wei Zhang, Shaojiao Wang, Rujiang Zhou, Xuechun Xia, Zhengju Yao, Pengxiao Li, Xiaodong Zhao, Jiqiu Wang and Xizhi Guo

There were errors in *Development* (2022) **149**, dev200260 (doi:10.1242/dev.200260).

The location labels in Fig. 3D were incorrect. The corrected and original panels are shown below.

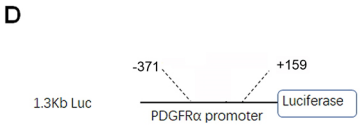

Fig. 3. (corrected). FOXP4 controls beige adipocyte differentiation by regulating *Pdgfra* transcription. (D) One putative FOXP4 binding site was detected −107 bp upstream of the *Pdgfra* gene transcription start site (TSS). Luciferase reporter assay validated the repressive activity of Foxp4 protein in *Pdgfra* gene transcription in HEK293T cells.

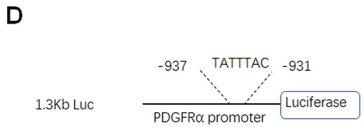

Fig. 3. (original). FOXP4 controls beige adipocyte differentiation by regulating *Pdgfra* transcription. (D) One putative FOXP4 binding site was detected −937 bp upstream of the *Pdgfra* gene transcription start site (TSS). Luciferase reporter assay validated the repressive activity of Foxp4 protein in *Pdgfra* gene transcription in HEK293T cells.

The legend for Fig. 7B quoted an incorrect target number. The corrected and original legends are shown below.

Fig. 7. (corrected). FOXP4 directly regulates the expression of Cebpb and Pgc1a during beige adipocyte thermogenic activation. (B) Heatmap of the 22 putative FOXP4-targeted gene expressions from the experiment shown in A. Chromatin occupancy analysis of ChIP-seq was conducted for SVF-derived beige adipocytes with an anti-Foxp4 antibody and 22 common targets were detected to overlap with RNA-seq results.

Fig. 7. (original). FOXP4 directly regulates the expression of Cebpb and Pgc1a during beige adipocyte thermogenic activation. (B) Heatmap of the 22 putative FOXP4-targeted gene expressions from the experiment shown in A. Chromatin occupancy analysis of ChIP-seq was conducted for SVF-derived beige adipocytes with an anti-Foxp4 antibody. Five common targets were detected to overlap with RNA-seq results.

In Fig. S6C, the heatmap was incorrect. The corrected and original figures are shown below.

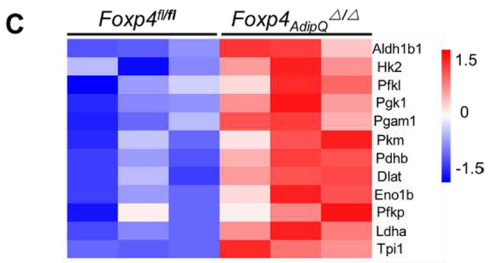

Fig. S6. (corrected). BAT thermogenesis in *Foxp4*$_{AdipQ}^{\Delta/\Delta}$ mice upon cold exposure. (C) Heatmap depicting the mRNA levels of glycolytic genes in beige adipocytes from sWAT in *Foxp4*$_{AdipQ}^{\Delta/\Delta}$ mice after one-week cold exposure at 4°C.

Development (2022) 149, dev200853. doi:10.1242/dev.200853

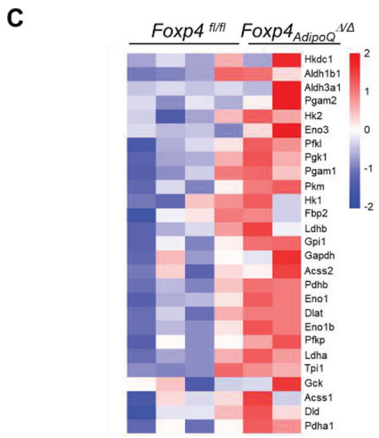

Fig. S6. (original). BAT thermogenesis in *Foxp4*$_{AdipoQ}^{Δ/Δ}$ mice upon cold exposure. (C) Heatmap depicting the mRNA levels of glycolytic genes in beige adipocytes from sWAT in *Foxp4*$_{AdipoQ}^{Δ/Δ}$ mice after one-week cold exposure at 4°C.

In Fig. S8, a panel was removed, so both the figure and legend have been updated. The corrected and original figures are shown below.

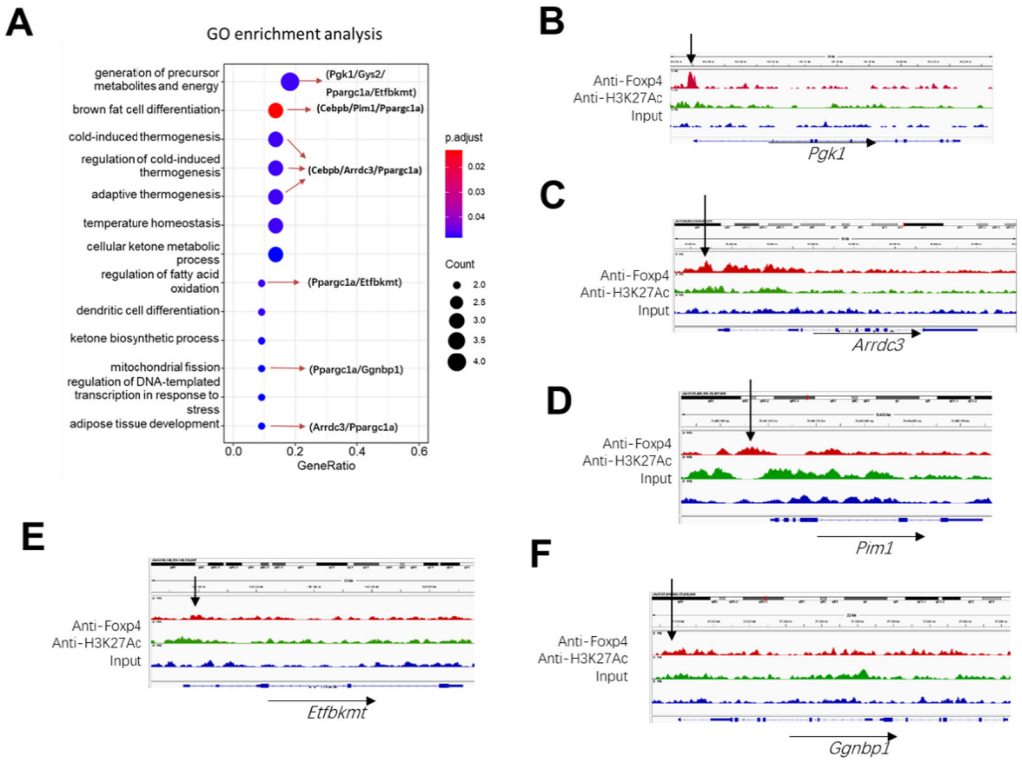

Fig. S8. (corrected). Crossover examinations of RNA-2 seq and ChIP-seq data to identify putative FOXP4 targeting genes. (A) GO enrichment analysis for several putative FOXP4-targeting genes. (B-F) ChIP-seq profile showed the FOXP4 binding sites (black arrows) within *Pgk1*, *Arrdc3*, *Pim1*, *Etfbkmt*, *Ggnbp1* gene regions.

Development (2022) 149, dev200853. doi:10.1242/dev.200853

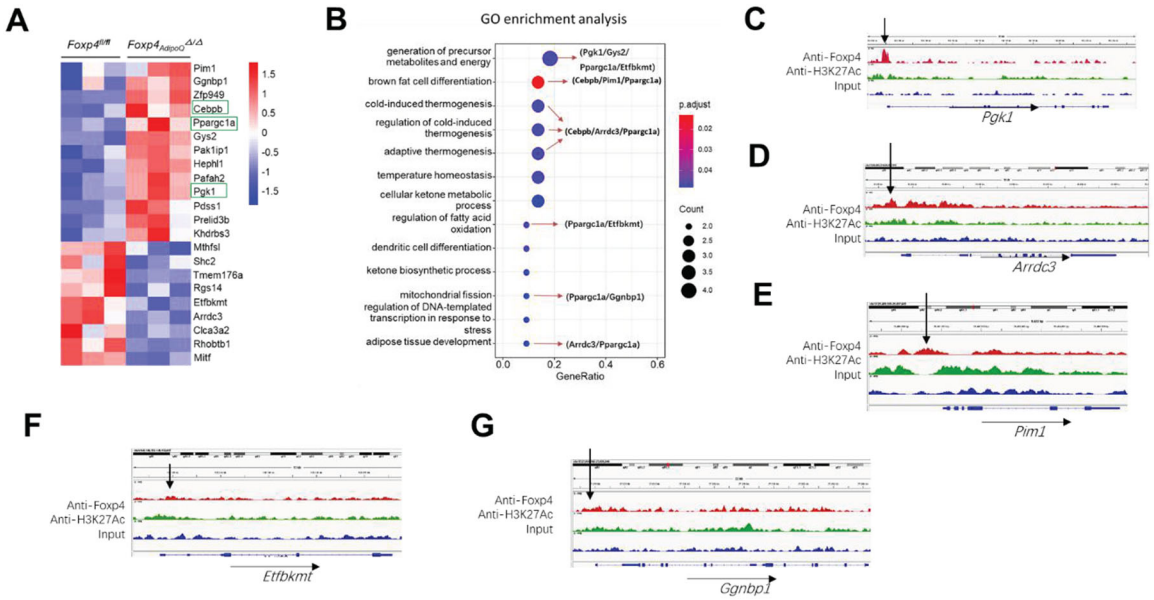

Fig. S8. (original). Crossover examinations of RNA-seq and ChIP-seq data to identify putative FOXP4 targeting genes. (A) Heatmap of thermogenic marker gene expressions by RNA-seq analysis in sWAT of *Foxp4*$_{AdipQ}^{\Delta/\Delta}$ mice under one-week 4°C challenge. (B) GO enrichment analysis for several putative FOXP4-targeting genes. (C-G) ChIP-seq profile showed the FOXP4 binding sites (black arrows) within *Pgk1*, *Arrdc3*, *Pim1*, *Etfbkmt*, *Ggnbp1* gene regions.

Also, some values for *n* have been replaced in the updated Supplementary information.

Fig. S3B
Corrected
(B) Assessment of *Foxp4* mRNA expression in BAT and sWAT from mice by qPCR. n, 3~5.
Original
(B) Assessment of *Foxp4* mRNA expression in BAT and sWAT from mice by qPCR. n, 3.

Fig S3H
Corrected
(H) Oxygen consumption rate (OCR) was measured for brown adipocytes from (F). Uncoupled respiration was recorded after oligomycin inhibition of 1 ATP synthesis, and maximal respiration following stimulation with carbonyl cyanide 4-(trifluoromethoxy) phenylhydrazone (FCCP). n, 7.
Original
(H) Oxygen consumption rate (OCR) was measured for brown adipocytes from (F). Uncoupled respiration was recorded after oligomycin inhibition of ATP synthesis, and maximal respiration following stimulation with carbonyl cyanide 4-(trifluoromethoxy) phenylhydrazone (FCCP). n, 3.

Fig S3I
Corrected
(I) Quantitative analysis of basal and uncoupled OCR in (H). n, 7.
Original
(I) Quantitative analysis of basal and uncoupled OCR in (H). n, 3.

Fig S7B,D
Corrected
(B,D) qPCR analysis for thermogenic gene expressions in BAT (B) and sWAT (D) from CL-316,243-stimulated mice. n, 3.
Original
(B,D) qPCR analysis for thermogenic gene expressions in BAT (B) and sWAT (D) from CL-316,243-stimulated mice. n, 5.

Both the online full text and PDF versions of the paper have been corrected. We apologise to the readers for these errors and any inconvenience they may have caused.

© 2022. Published by The Company of Biologists Ltd | Development (2022) 149, dev200260. doi:10.1242/dev.200260

RESEARCH ARTICLE

FOXP4 differentially controls cold-induced beige adipocyte differentiation and thermogenesis

Fuhua Wang[1], Shuqin Xu[1], Tienan Chen[1], Shifeng Ling[1], Wei Zhang[1], Shaojiao Wang[1], Rujiang Zhou[1], Xuechun Xia[1], Zhengju Yao[1], Pengxiao Li[2], Xiaodong Zhao[2], Jiqiu Wang[3] and Xizhi Guo[1,*]

ABSTRACT

Beige adipocytes have a discrete developmental origin and possess notable plasticity in their thermogenic capacity in response to various environmental cues, but the transcriptional machinery controlling beige adipocyte development and thermogenesis remains largely unknown. By analyzing beige adipocyte-specific knockout mice, we identified a transcription factor, forkhead box P4 (FOXP4), that differentially governs beige adipocyte differentiation and activation. Depletion of *Foxp4* in progenitor cells impaired beige cell early differentiation. However, we observed that ablation of *Foxp4* in differentiated adipocytes profoundly potentiated their thermogenesis capacity upon cold exposure. Of note, the outcome of *Foxp4* deficiency on UCP1-mediated thermogenesis was confined to beige adipocytes, rather than to brown adipocytes. Taken together, we suggest that FOXP4 primes beige adipocyte early differentiation, but attenuates their activation by potent transcriptional repression of the thermogenic program.

KEY WORDS: Beige adipocyte, Cell differentiation, Thermogenesis, Transcription factor, FOXP4

INTRODUCTION

Beige adipocytes, a population of thermogenic adipocytes distinct from brown adipocytes, have recently attracted mainstream attention. Their relevance to adult humans holds promise as a new therapeutic target in combating obesity and other metabolic disorders. Beige adipocytes emerge within white adipose tissue (WAT) depots in response to various environmental cues, including chronic cold acclimatization, exercise, β3-adrenergic receptor (AR) agonists, cancer cachexia, and tissue injury (Barbatelli et al., 2010; Rosenwald et al., 2013). As with classical brown adipocytes, beige adipocytes present with multilocular morphology and produce heat mainly through UCP1-mediated thermogenesis. Lineage-tracing studies have demonstrated that beige adipocytes consist of heterogeneous subpopulations of distinct origins depending on the nature of external induction stimuli (Berry et al., 2016). For example, beige adipocytes originate either from PDGFRα$^+$ stromal progenitor cells (Han et al., 2021; Lee et al., 2015, 2012), or from mural perivascular cells when targeted by *SMA-CreERT* (Long et al., 2014). These two beige progenitor populations are not mutually exclusive. A recent study noted that PDGFRα$^+$ progenitor cells are required for developmental adipogenesis, but not for adult beige adipogenesis (Shin et al., 2020). Further evidence showed that beige precursor cells are a population distinct from brown or white fat precursors with selective cell-surface markers, including CD81 (Oguri et al., 2020) and CD137 (TNFRSF9) (Wu et al., 2012).

Following cell fate determination and differentiation, beige adipocytes possess inducible and reversible thermogenic capacity, as well as plasticity in cellular morphology in response to environmental stimuli (Paulo and Wang, 2019). The first wave of *de novo* beige adipocytes express UCP1 with multilocular morphology. They appear in WAT of mice independently of temperature conditions at the peri-weaning stage of development (Wu et al., 2020). At the adult stage, these beige adipocytes regress, lose UCP1 expression and are morphologically identical to white adipocytes at room temperature. The dormant beige adipocytes can reappear in response to cold challenge, and reverse back to white-like cellular morphology in conditions of re-warming or withdrawal of β3-AR agonist (Roh et al., 2018; Rosenwald et al., 2013). Previous studies have proposed that cold-induced beige adipocytes predominantly arise from transdifferentiation of pre-existing white adipocytes (Barbatelli et al., 2010; Cattaneo et al., 2020; Rosenwald et al., 2013). However, this view requires cautious assessment because of the current technical limitations to determine how many of those pre-existing 'white' adipocytes are *de facto* latent beige adipocytes with UCP1$^+$ history. Of note, the conversion between thermogenically latent and active states in beige fat cells may be attributed to reversible processes of mitochondrial biogenesis and clearance (Altshuler-Keylin et al., 2016), as well as to chromatin reprogramming and function of specific transcriptional machinery (Roh et al., 2018).

Despite these differences in developmental origins and physiological functions of brown, beige and white adipocytes, these cell types share a similar transcriptional cascade that controls the process of fat cell differentiation. Several factors are commonly employed by both brown and beige adipocytes, including Cebpα/β-PPARγ cascades for early cell fate commitment and differentiation, as well as activators of EBF2, Prdm16 and PGC1α (PPARGC1α) for thermogenesis (Shapira and Seale, 2019; Wang and Seale, 2016). However, as mentioned above, beige adipocyte plasticity in cell differentiation and thermogenesis involves cell-specific changes in morphology, transcription and the chromatin landscape. In contrast to our significant understanding of brown adipocyte transcription, the beige-selective regulatory machinery remains largely unclear.

Forkhead box P4 (FOXP4) typically functions as a transcription factor that regulates islet α cell proliferation (Spaeth et al., 2015), breast cancer invasion (Ma and Zhang, 2019) and speech/language (Snijders Blok et al., 2021). Our previous studies have shown that

[1]Bio-X-Renji Hospital Research Center, Renji Hospital, School of Medicine, Shanghai Jiao Tong University, Shanghai, 200240, China. [2]Shanghai Center for Systems Biomedicine, Shanghai Jiao Tong University, Shanghai, 200240, China. [3]Department of Endocrinology and Metabolism, Ruijin Hospital, Shanghai Jiao Tong University School of Medicine, Shanghai, 200025, China.

*Author for correspondence (xzguo2005@sjtu.edu.cn)

F.W., 0000-0002-9383-7656; S.X., 0000-0003-0180-9680; T.C., 0000-0003-2457-4685; S.L., 0000-0001-8388-0688; P.L., 0000-0003-3519-141X; X.G., 0000-0001-8047-6049

Handling Editor: Haruhiko Koseki
Received 12 October 2021; Accepted 7 March 2022

Development (2022) 149, dev200260. doi:10.1242/dev.200260

FOXP4 also controls endochondral ossification in a complex with FOXP1 and FOXP2 (Zhao et al., 2015). In this study, we employed *SMA-Cre*^{ERT} and *AdipoQ-Cre* mice to knock out *Foxp4* in beige precursors and differentiated beige cells, respectively. Inactivation of *Foxp4* in progenitor cells impaired beige fat cell differentiation. In contrast, *Foxp4* deficiency in differentiated beige adipocytes exacerbated their cold-induced thermogenesis response. Mechanistically, we found that FOXP4 directly repressed transcription of *Pdgfra*, *Pgc1a* and *Cebpb*, thereby acting as a transcriptional 'brake' on these crucial components of beige adipocyte regulation. Together, our results suggest that FOXP4 not only primes early cell fate commitment of beige adipocytes, but also attenuates their cold-induced thermogenesis response.

RESULTS

Dynamic expression of *Foxp4* during beige adipocyte differentiation

To investigate the expression pattern of FOXP4 in adipose tissues, two representative subpopulations of adipocytes, interscapular brown adipose tissues (BAT) and subcutaneous white adipose tissues (sWAT), were obtained from 8-week-old wild-type C57BL/6J mice that were housed at room temperature (23°C). High levels of FOXP4 expression were detected within brown and white adipocytes by immunofluorescence analyses (Fig. 1A). Next, stromal vascular fraction (SVF) cells isolated from sWAT of wild-type mice were induced to beige adipocytes *in vitro* by culturing in beige adipogenic media for 7 days. As expected, *Pparg* and *Ucp1* expression levels were elevated during beige adipocyte differentiation, whereas *Foxp4* expression peaked at day 2 of induction and declined swiftly thereafter (Fig. 1B). In addition, western blotting and qPCR analysis revealed that FOXP4 expression in BAT and sWAT was slightly increased in response to cold exposure (Fig. S1A,B). These dynamic alterations in expression indicate a phase-specific function of FOXP4 during beige adipocyte differentiation.

Ablation of *Foxp4* impairs beige adipocyte early differentiation

To investigate the function of FOXP4 in brown/beige adipocyte differentiation, we first transfected the SVF cells from *Foxp4*$^{fl/fl}$ sWAT with either retroviral *pMSCV-Cre* or, as a control, retroviral *pMSCV-GFP*. This approach allowed us to achieve efficient and extensive inactivation of *Foxp4* in adipocyte progenitors. Minor alterations in brown adipocyte differentiation and thermogenesis were detected in BAT-SVF cells with *Foxp4* deficiency (designated *Foxp4*$_{pMSCV}^{\Delta/\Delta}$) (Fig. 1C,D). In contrast, beige adipocyte differentiation in *Foxp4*-deficient sWAT-SVF cells was impaired, as evidenced by Oil Red O staining and downregulation of a set of thermogenic (*Pparg*, *Pgc1a*, *Adrb3*, *Ucp1*, *Cidea*, *Dio2*, *Elovl3*) and beige-elective signature genes (*CD137*, *Slc27a1*) (Fig. 1E-G). Of note, deletion of *Foxp4* by *pMSCV-Cre* had little effect on white adipogenesis, as evidenced by Oil Red O staining and qPCR based on sWAT-SVF adipogenic cultures without triiodothyronine (T3) and thiazolidinediones (Fig. S1C,D). Thus, FOXP4 expression is required for beige adipocyte early differentiation from stromal progenitor cells.

A major proportion of adult beige adipocytes is reported to be derived from mural progenitor cells within sWAT, which could be selectively and conditionally targeted by *SMA-Cre*^{ERT} (Long et al., 2014). Unfortunately, when *Foxp4* was inactivated by *SMA-Cre*, the knockout mice showed defects in postnatal development and growth (data not shown). Therefore, tamoxifen (TM)-inducible *Foxp4* conditional knockout mice at adult stage (hereafter designated *Foxp4*$_{Sma}^{Ert\Delta/\Delta}$) were generated by crossing *Foxp4*$^{fl/fl}$ with *SMA-Cre*^{ERT} mice. SVF cells obtained from sWAT of *Foxp4*$_{Sma}^{Ert\Delta/\Delta}$ were maintained for 2 days within cultures with 4-OH TM, followed by another 8 days in beige adipogenic differentiation (Fig. 2A). Beige cell differentiation was impaired following loss of *Foxp4*, as evidenced by Oil Red O staining (Fig. 2B). In addition, we observed decreased expression levels of *Foxp4* (Fig. 2C), beige-specific markers (*CD137*, *Klhl13*, *Slc27a1*) (Fig. 2D) and thermogenic markers [*Ucp1*, *Cidea*, *Elovl3*, *Cox2* (*Ptgs2*), *Cox4i1*, *Cox5b*, *Cox7a*] genes (Fig. 2E). The defects of beige cell differentiation may stem from perturbed *de novo* biogenesis. We next tracked PDGFRα^{+} stem cell antigen 1 (Sca1)$^{+}$ adipocyte progenitor cells (APCs) within WAT-SVF 48 h post-TM administration by flow cytometry (FACS) as described previously (Berry and Rodeheffer, 2013; Lee et al., 2015). The frequency of APCs [defined as CD31 (Pecam1)$^{-}$CD45 (Ptprc)$^{-}$PDGFRα^{+}Sca1^{+}] was relatively lower in SVF cells of *Foxp4*$_{Sma}^{Ert\Delta/\Delta}$ compared with those of *Foxp4*$^{fl/fl}$ (Fig. 2F,G).

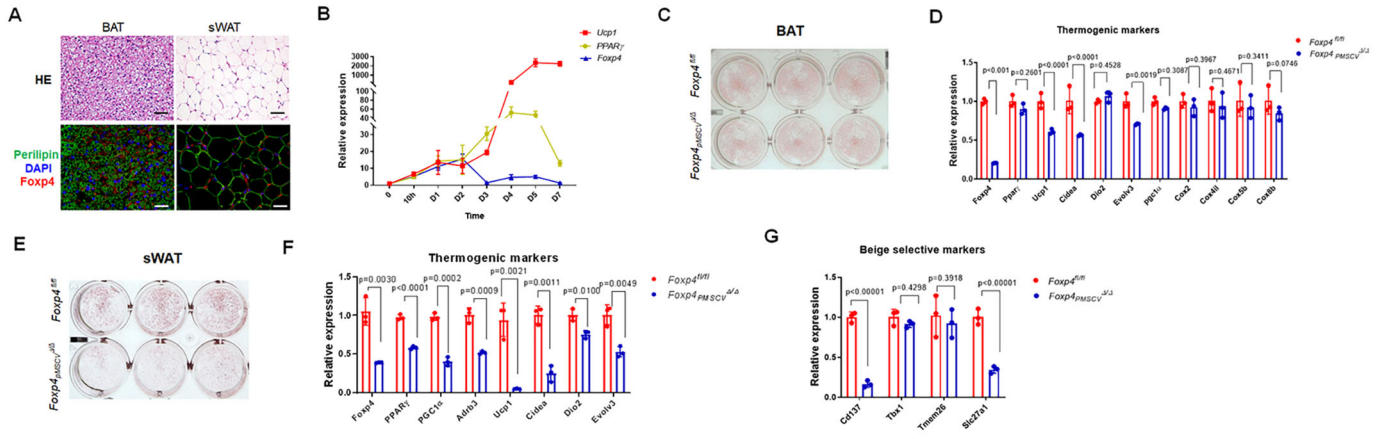

Fig. 1. Ablation of *Foxp4* impairs beige adipocyte differentiation. (A) HE staining and immunofluorescence detection of FOXP4 on sections from BAT and sWAT of 2-month-old wild-type mice. DAPI was used as nuclear stain and perilipin to stain lipid membranes. Scale bars: 100 µm. Three independent experiments were replicated. (B) mRNA levels of *Foxp4*, *Pparg* and *Ucp1* during culture courses of beige adipocyte differentiation derived from the stromal vascular fraction (SVF) of sWAT depot. *n*=3. D, day of culture. (C) Oil Red O staining to visualize 8-day brown adipocyte differentiation from *pMSCV-Cre*-transfected SVF of BAT from *Foxp4*$^{fl/fl}$ mice. Three independent experiments were replicated. (D) mRNA levels of *Foxp4* and thermogenic and brown-selective markers for the cells shown in C. *n*=3. (E) Oil Red O staining to visualize 8-day brown adipocyte differentiation from *pMSCV-Cre*-transfected SVF of sWAT from *Foxp4*$^{fl/fl}$ mice. Three independent experiments were replicated. (F,G) mRNA levels of thermogenic and beige-selective markers in the cells shown in E. *n*=3.

Development (2022) 149, dev200260. doi:10.1242/dev.200260

In addition, we administered three consecutive injections of TM to the *Foxp4*$_{Sma}^{ErtΔ/Δ}$ mice, cultured them for 2 weeks at room temperature and exposed them to cold (4°C) for 3 days before the SVF cells were harvested for FACS analysis (Fig. 2H). The knockout efficiency of FOXP4 in SVF cells was validated by western blot (Fig. S1E). *In vivo* FACS analysis confirmed the reduction of adipocyte progenitor cells (Fig. 2I). qPCR analysis also showed the relative downregulation of *Slc27a1* and *Tbx1*, two beige-selective marker genes (Fig. 2J). These observations indicate that FOXP4 inactivation decreases the APC population proportion, thus potentially impairing beige cell early differentiation.

FOXP4 regulates early adipocyte differentiation by directly controlling *Pdgfra* transcription

Interestingly, qPCR analysis revealed that an array of collagen fibril-related transcripts was relatively enriched in *Foxp4*$_{pMSCV}^{Δ/Δ}$ beige cells compared with controls. Elevated expression levels of several of these pro-fibrotic genes (*Col1a1*, *Col3a1*, *Col4a1*, *Col6a3*, *Mmp2*, *Timp1*, *CD9*) were detected in mutant beige cells (Fig. S2A). Accordingly, similar alterations of fibroblast marker genes were observed in beige cells obtained from sWAT-SVF of *Foxp4*$_{Sma}^{ErtΔ/Δ}$ mice following *Foxp4* inactivation induced by TM (Fig. S2B). These observations indicate that more *Foxp4*-deficient beige progenitor cells are arrested at fibroblast progenitor state.

PDGFRα^{+} stromal progenitor cells also give rise to beige adipocytes during early development (Gao et al., 2018). Activation of the PDGFRα pathway can also perturb the differentiation of beige adipocytes (Shin et al., 2020; Sun et al., 2017). We then investigated the impact of FOXP4 on *Pdgfra* gene transcription. qPCR analysis revealed that *Pdgfra* transcripts were increased in beige progenitor cells from *Foxp4*$_{pMSCV}^{Δ/Δ}$ or in *Foxp4*$_{Sma}^{ErtΔ/Δ}$ mice (Fig. 3A), as was the PDGFRα protein level (Fig. 3B). In addition, chromatin immunoprecipitation and sequencing (ChIP-seq) analysis of SVF progenitor cells detected relatively high enrichment of FOXP4-binding sites within the promoter region of *Pdgfra* (Fig. 3C, arrow). A putative FOXP4-binding site was detected at −107 upstream of the *Pdgfra* transcription start site (Fig. 3D). Luciferase reporter assays employing a *Pdgfra* promoter-driven luciferase as substrate validated that FOXP4 repressed transcription of *Pdgfra* in HEK293T cells (Fig. 3D). On the other hand, overexpression of FOXP4 by *pMSCV* retrovirus repressed PDGFRa expression in SVF progenitor cells (Fig. 3E). Together, these data suggest that FOXP4 controls the early differentiation of beige adipocytes by directly modulating *Pdgfra* transcription.

Ablation of *Foxp4* modestly augments juvenile and mature beige adipocyte thermogenesis

The first wave of *de novo* beige adipocyte biogenesis and UCP1 activation occurs within sWAT at the peri-weaning stage independently of temperature conditions (Wang et al., 2017; Wu

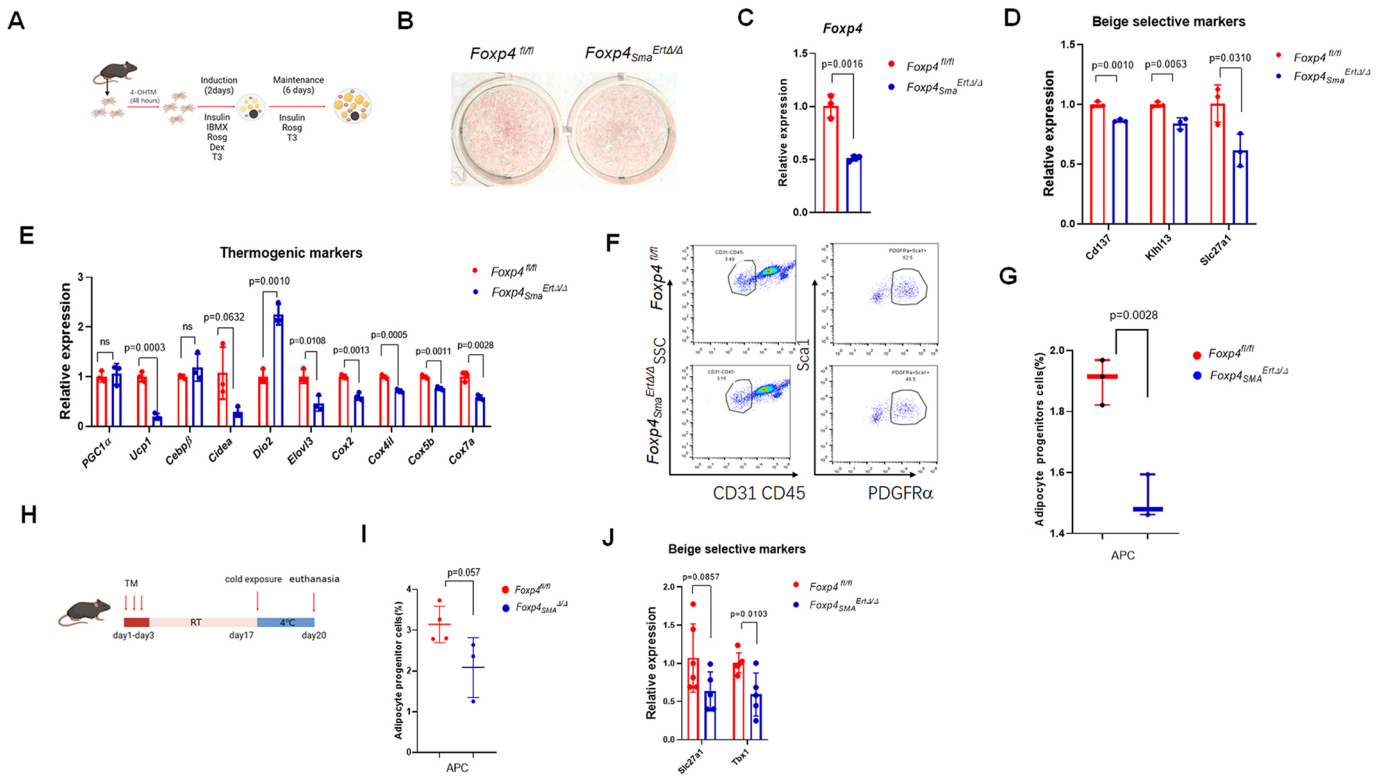

Fig. 2. *Foxp4* deficiency disrupts beige adipocyte differentiation from SMA^{+} progenitor cells. (A) Schematic depicting the treatment of sWAT-SVF cells with 4-OH TM 24-h post-isolation and cultures to induce *Foxp4* knockout in beige cells, which were designated as *Foxp4*$^{fl/fl}$ and *Foxp4*$_{Sma}^{ErtΔ/Δ}$. Subsequently, these precursor cells underwent 8-day beige induction cultures. (B) Oil Red O staining of the SVF-derived beige adipocytes shown in A. Three independent experiments were replicated. (C-E) mRNA levels of *Foxp4* and beige-selective and thermogenic markers in the cells shown in B. *n*=3. (F) Flow cytograms showing expression of PDGFRα and Sca1 in adipocyte progenitor cells (APC, CD31^{-}CD45^{-}PDGFRα^{+}Sca1^{+}) 24-h post TM induction in SVF cell cultures. (G) Quantitative analysis of the proportion of adipocyte progenitor cells in the experiment shown in F. *n*=3. (H) Schematic depicting the administration of three consecutive TM injections to *Foxp4*$^{fl/fl}$ and *Foxp4*$_{Sma}^{ErtΔ/Δ}$, and the culture of mice for 2 weeks at room temperature followed by 3 days at 4°C before SVF were harvested for FACS. (I) Quantitative analysis for proportion of adipocyte progenitor cells in H. *n*=3 or 4. (J) mRNA levels of beige selective markers in cells from I. *n*=5.

Development (2022) 149, dev200260. doi:10.1242/dev.200260

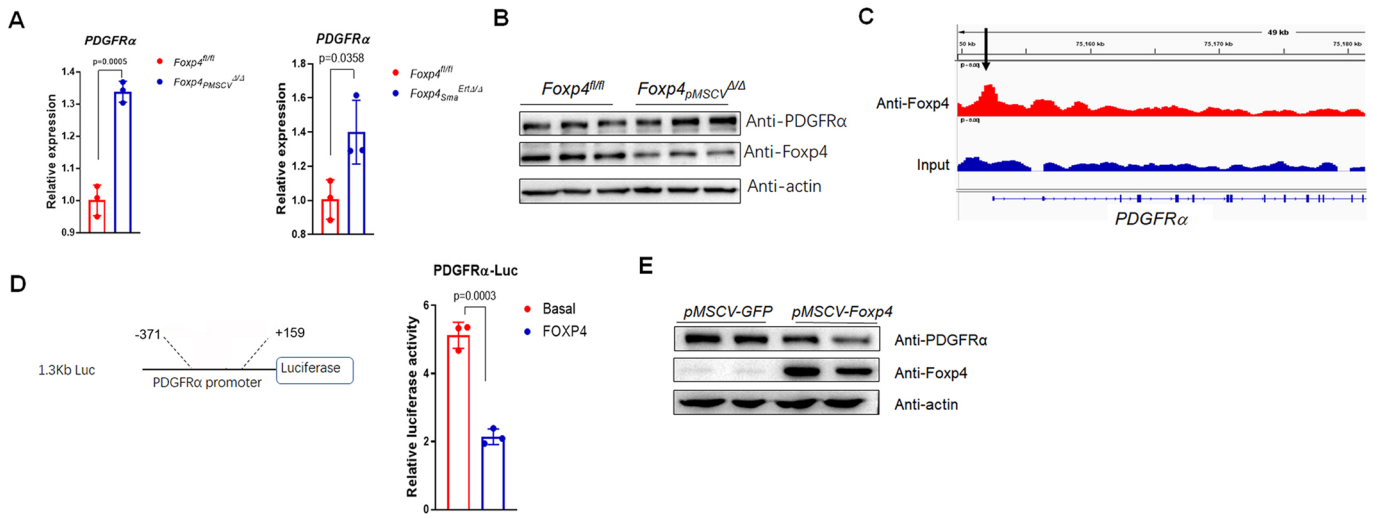

Fig. 3. FOXP4 controls beige adipocyte differentiation by regulating *Pdgfra* transcription. (A) qPCR validated the increased *Pdgfra* expression levels in beige adipocytes as a result of *Foxp4* deficiency by *pMSCV-Cre* or *SMA-CreER*. *n*=3. (B) Western blot for expression of PDGFRα and FOXP4 in beige progenitor cells with *Foxp4* deficiency by *pMSCV-Cre*. SVF cells were harvested for western blot 2 days post cell expansion culture. Three independent experiments were replicated. (C) Chromatin occupancy analysis by ChIP-seq showed the relative enrichment of Foxp4-binding sites (black arrow) upstream of the *Pdgfra* gene promoter region, based on beige adipocytes derived from SVF of wild-type sWAT. (D) One putative FOXP4 binding site was detected −107 bp upstream of the *Pdgfra* gene transcription start site (TSS). Luciferase reporter assay validated the repressive activity of Foxp4 protein in *Pdgfra* gene transcription in HEK293T cells. (E) Western blot for expression of PDGFRα and FOXP4 in beige progenitor cells with *Foxp4* overexpression by *pMSCV-GFP* or *pMSCV-Foxp4*. *n*=3.

et al., 2020). To evaluate the potential impact of *Foxp4* deficiency on beige adipocyte thermogenesis, we eliminated *Foxp4* in differentiated adipocytes with *AdipoQ-Cre* (Eguchi et al., 2011), hereafter designated $Foxp4_{AdipoQ}^{\Delta/\Delta}$. We confirmed that FOXP4 was efficiently reduced at the mRNA and protein levels in BAT and sWAT from $Foxp4_{AdipoQ}^{\Delta/\Delta}$ mice (Fig. S3A-C). $Foxp4_{AdipoQ}^{\Delta/\Delta}$ mice appeared relatively normal in size and in the appearance of fat depots of BAT and sWAT at 3 weeks of age (Fig. 4A,B). Hematoxylin and Eosin (HE) staining and immunohistochemistry (IHC) analysis revealed that higher numbers of $UCP1^{+}$ beige adipocytes resided in sWAT from $Foxp4_{AdipoQ}^{\Delta/\Delta}$ knockout mice than in controls (Fig. 4C). Consistent with that observation, qPCR analysis confirmed the upregulation of a set of thermogenic and mitochondrial signature genes (*Dio2*, *Elovl3*, *Pgc1a*, *Ucp1*, *Cox2*, *Cox4i1*, *Cox5b*, *Cox8b*) (Fig. 4D,E). However, the expression of several beige-selective marker genes (*CD137*, *CD40*, *Klhl13*, *Tbx1*) showed no obvious increases (Fig. 4F). These observations suggest that FOXP4 boosts juvenile beige adipocyte activation, but has little effect on their early biogenesis.

The transcriptional pathway underlying adult beige cell differentiation and thermogenic activation is distinct from that of the juvenile at the peri-weaning stage (Wu et al., 2020).

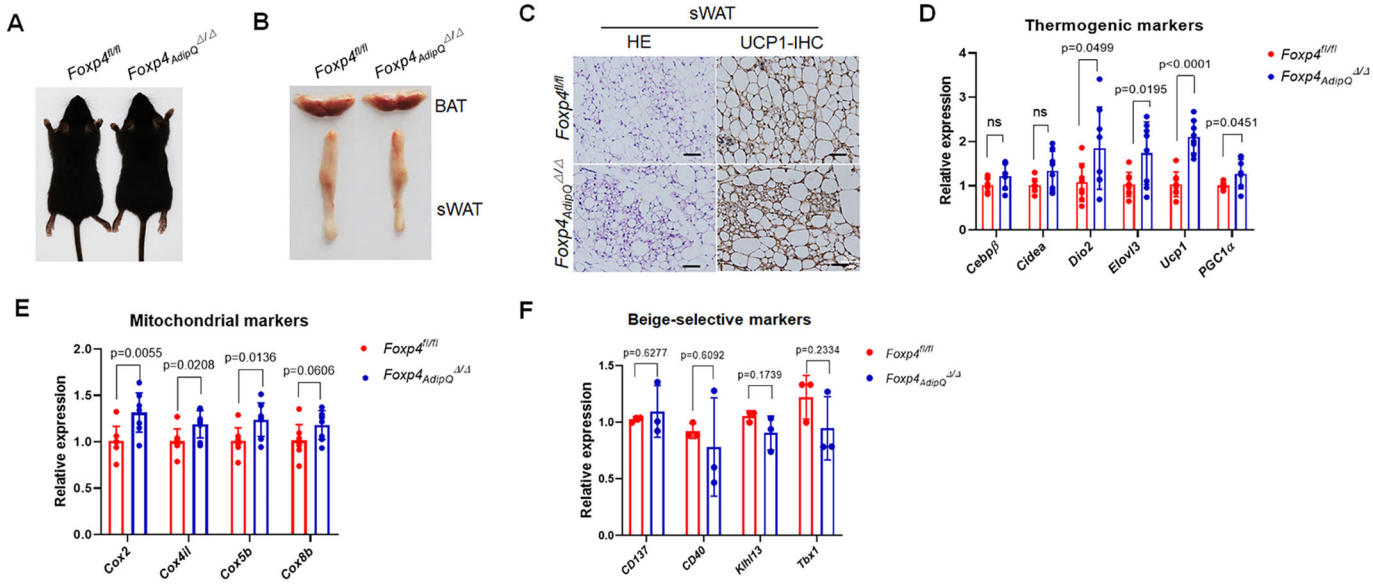

Fig. 4. *Foxp4* deletion mildly augments beige adipocytes thermogenesis at the peri-weaning stage. (A) Dorsal view of representative $Foxp4^{fl/fl}$ and $Foxp4_{AdipoQ}^{\Delta/\Delta}$ mice at 3 weeks old. (B) Gross morphology of BAT and sWAT depot of the mice shown in A. (C) HE and immunohistochemical staining (IHC) for UCP1 on sWAT sections from $Foxp4_{AdipoQ}^{\Delta/\Delta}$ mice. Three independent experiments were replicated. Scale bars: 100 µm. (D,E) mRNA levels of thermogenic and mitochondrial markers in sWAT. *n*=8. (F) qPCR validated the relative normal expression levels of beige-selective marker genes in sWAT from $Foxp4_{AdipoQ}^{\Delta/\Delta}$ mice. *n*=3.

Development (2022) 149, dev200260. doi:10.1242/dev.200260

Foxp4$_{AdipQ}^{\Delta/\Delta}$ knockout mice appeared normal in size, weight and adiposity compared with controls at adult stages (Fig. 5A). They were modestly smaller at 5 months (Fig. 5B). Accordantly, the thermogenic program in the BAT of *Foxp4*$_{AdipQ}^{\Delta/\Delta}$ mice did not appear to be activated at ambient temperature (20-22°C), as indicated by HE staining and IHC, as well as by qPCR analysis of a set of thermogenic marker transcripts (Fig. S3D,E). Indirect calorimetry analysis by CLAMS (Comprehensive Lab Animal Monitoring System) revealed that *Foxp4* loss had no impact on O_2 or CO_2 consumption, as well as on energy expenditure following identical diet and locomotor activity as controls at 20~22°C (Fig. S4). In contrast, thermogenic activation of beige adipocytes was mildly exacerbated in sWAT of *Foxp4*$_{AdipQ}^{\Delta/\Delta}$ mice, as evidenced by relatively enriched levels of UCP1^{+} adipocytes and by upregulation of thermogenic or mitochondrial signature genes (*Pparg*, *Dio2*, *Cidea*, *Ucp1*, *Cox2*, *Cox4i1*, *Cox5b*, *Cox8b*) (Fig. 5C,D). We conclude from these analyses that loss of FOXP4 results in modest augmentation of thermogenesis in beige adipocytes at ambient temperature.

Foxp4 deficiency protects mice from high fat diet-induced obesity

Beige adipocyte thermogenesis could combat obesity in human (Lidell et al., 2013). To examine the impact of *Foxp4* deficiency on long-term adipose tissue metabolism, mice were fed a high-fat diet (HFD) for 3 months. We observed that *Foxp4*$_{AdipQ}^{\Delta/\Delta}$ mice were leaner in body, with fewer adipose depots (Fig. S5A,B), and gained less body weight and adiposity than littermates after 12 weeks of HFD feeding starting at the age of 2 months (Fig. S5C). *Foxp4*$_{AdipQ}^{\Delta/\Delta}$ mutant mice also retained more efficient glucose tolerance following HFD feeding, as evidenced by glucose tolerance test scores (Fig. S5D). Of note, as previously mentioned, UCP1-mediated beige thermogenesis was mildly diminished in *Foxp4*$_{AdipQ}^{\Delta/\Delta}$ mutant mice at room temperature (Figs 4C,D and 5C,D), which may undermine the protective effect against HFD-induced obesity provided by *Foxp4* deficiency.

FOXP4 suppresses beige adipocyte thermogenesis cell-autonomously

To examine a potential cell-autonomous effect of FOXP4 on beige adipocyte energy metabolism, SVF cells were isolated from sWAT depots of *Foxp4*$_{AdipQ}^{\Delta/\Delta}$ and control mice and then induced for beige adipocyte differentiation *in vitro*. We observed advanced beige adipocyte thermogenesis in *Foxp4*-deficient SVF progenitors, as evaluated by elevated mRNA levels of a set of thermogenic genes (*Cidea*, *Pgc1a*, *Ucp1*, *Cox2*, *Cox7a1*, *Cox5b*, *Cox8b*) (Fig. 5E,F). In addition, oxygen consumption rates (OCR) of beige adipocytes from *Foxp4*$_{AdipQ}^{\Delta/\Delta}$ mutant mice exhibited higher basal and uncoupled OCR compared with controls (Fig. 5G,H). These results indicate that loss of FOXP4 led to elevated mitochondrial respiration. The thermogenic potency of SVF-derived brown adipocyte was also potentiated in *Foxp4*-deficient mice, as evidenced by qPCR and OCR analyses (Fig. S3F-I). This line of evidence indicates that FOXP4 suppresses beige adipocyte thermogenesis in a cell-autonomous manner.

Foxp4 depletion exacerbates cold-induced beige adipocyte thermogenesis *in vivo*

We demonstrated that beige adipocytes could be mildly activated within sWAT at room temperature at the adult stage. We then examined beige adipocyte thermogenesis and activation in *Foxp4*$_{AdipQ}^{\Delta/\Delta}$ mice under cold conditions. Compared with controls, *Foxp4* knockout mice had relatively higher rectal temperature during a 6-h 4°C exposure (Fig. 6A). *Foxp4*$_{AdipQ}^{\Delta/\Delta}$ mice also displayed a 'browning' feature of sWAT after 1 week at 4°C (Fig. 6B). This result was consistent with HE staining and IHC results demonstrating higher levels of UCP1^{+} beige adipocytes (Fig. 6C). Elevated beige adipocyte thermogenesis was validated by RT-qPCR analysis of signature genes (*Cidea*, *Dio2*, *Elovl3*, *Pgc1a*, *Ucp1*, *Cox2*, *Cox5b*, *Cox8b*) (Fig. 6D). However, long-term cold exposure had no significant effect on beige adipocyte *de novo* biogenesis in mutant mice, as evidenced by compromised levels of beige signature genes (*Klhl13*, *Slc27a1*, *Tbx1*, *CD137*)

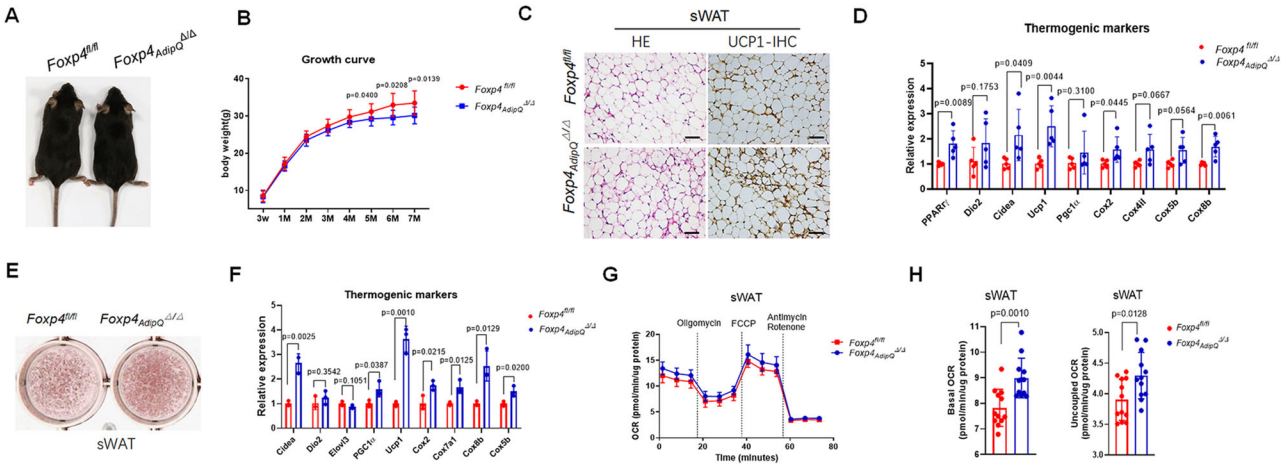

Fig. 5. FOXP4 cell-autonomously represses beige adipocytes thermogenesis. (A) Representative dorsal view of *Foxp4*$^{fl/fl}$ and *Foxp4*$_{AdipQ}^{\Delta/\Delta}$ mice at 2 months old. (B) Growth curve showing that body weights were mildly decreased in *Foxp4*$_{AdipQ}^{\Delta/\Delta}$ mice compared with *Foxp4*$^{fl/fl}$ control mice from the age of 5 months. *n*=8-12. (C) HE and IHC staining for UCP1 protein on sWAT sections from *Foxp4*$_{AdipQ}^{\Delta/\Delta}$ mice at 2 months old. Scale bars: 100 µm. Three independent experiments were replicated. (D) mRNA levels of a set of thermogenic genes in sWAT of *Foxp4*$_{AdipQ}^{\Delta/\Delta}$ mice. *n*=5. (E) Oil Red O staining of 8 day post brown adipocyte differentiation from sWAT-SVF of *Foxp4*$^{fl/fl}$ and *Foxp4*$_{AdipQ}^{\Delta/\Delta}$ mice at the age of 8 weeks. Three independent experiments were replicated. (F) mRNA levels of thermogenic markers for the beige adipocytes shown in E. *n*=7. (G) Oxygen consumption rate (OCR) was measured for the beige adipocytes shown in E. Uncoupled respiration was recorded after oligomycin inhibition of ATP synthesis, and maximal respiration following stimulation with carbonyl cyanide 4-(trifluoromethoxy) phenylhydrazone (FCCP). *n*=15. (H) Quantitative analysis of basal and uncoupled OCR for the experiment shown in G. *n*=15.

Development (2022) 149, dev200260. doi:10.1242/dev.200260

(Fig. 6E). Consistent with these observations, transmission electronic microscopy (TEM) and qPCR analysis revealed relative enrichment of mitochondria within beige adipocytes of $Foxp4_{AdipQ}^{\Delta/\Delta}$ sWAT (Fig. 6F,G). We further observed that cold exposure had little effect on thermogenesis in the BAT of $Foxp4_{AdipQ}^{\Delta/\Delta}$ mice (Fig. S6A,B). Together, these results suggest that FOXP4 acts as a repressor of the thermogenic gene program in beige adipocytes.

Thermogenesis of beige adipocytes could also be activated by adrenergic signaling (Jiang et al., 2017). However, when treated with 7 consecutive daily injections of the β3-AR agonist CL-316,243 $Foxp4_{AdipQ}^{\Delta/\Delta}$ mice exhibited no evident activation of the thermogenic program and no increase in beige adipocyte biogenesis, as determined by HE staining, IHC and RT-qPCR analyses (Fig. S7). These findings suggest that FOXP4 controls cold-induced beige adipocyte activation through adrenergic-independent signaling.

FOXP4 attenuates beige adipocyte thermogenesis partially by repressing *Pgc1a* and *Cebpb* transcription

To explore the molecular mechanism underlying the impact of FOXP4 on beige adipocyte thermogenesis and activation, RNA-sequencing (RNA-seq) analysis was performed on beige adipocytes derived from sWAT-SVF of $Foxp4_{AdipQ}^{\Delta/\Delta}$ mice. As shown in Fig. 7A,B, expression of an array of thermogenic or mitochondrial gene markers was elevated in *Foxp4*-deficient beige adipocytes. Next, we conducted ChIP-seq analysis of SVF-induced beige adipocytes by employing anti-FOXP4 and anti-H3K27Ac antibodies for pulldowns. As shown in Fig. 7B, 22 common target genes were detected by both RNA-seq and ChIP-seq, including the classical thermogenic genes *Pgc1a* and *Cebpb*. Western blotting confirmed the upregulation of PGC1α, Cebpβ and UCP1 at the protein level under conditions of decreased FOXP4 (Fig. 7C). Promoter occupancy as determined by ChIP-seq validated the relative enrichment of FOXP4-binding sites within the chromatin of *Pgc1a* and *Cebpb* upstream promoter regions (Fig. 7D, arrows). In support of this, reporter assays employing a *Pgc1a* promoter-driven luciferase vector revealed that FOXP4 repressed the transactivation ability of PPARγ in 3T3-L1 cells (Fig. 7E). Moreover, an array of putative FOXP4-binding site-enriched genes, such as *Pgk1*, *Arrdc3*, *Pim1*, *Etfbkmt*, *Ggnbp1*, were altered in *Foxp4*-deficient beige adipocytes (Fig. 7B). Gene ontology enrichment analysis showed that they mostly function in energy metabolism, thermogenesis or mitochondrial metabolism (Fig. S8). These findings demonstrate that FOXP4 restrains beige adipocyte thermogenesis by directly repressing the thermogenic program, in particular the expression of *Pgc1a* and *Cebpb*.

DISCUSSION

Beige fat cells harbor distinctive molecular signatures from white and brown adipocytes during development. Once committed from progenitor cells, differentiated beige adipocytes demonstrate a

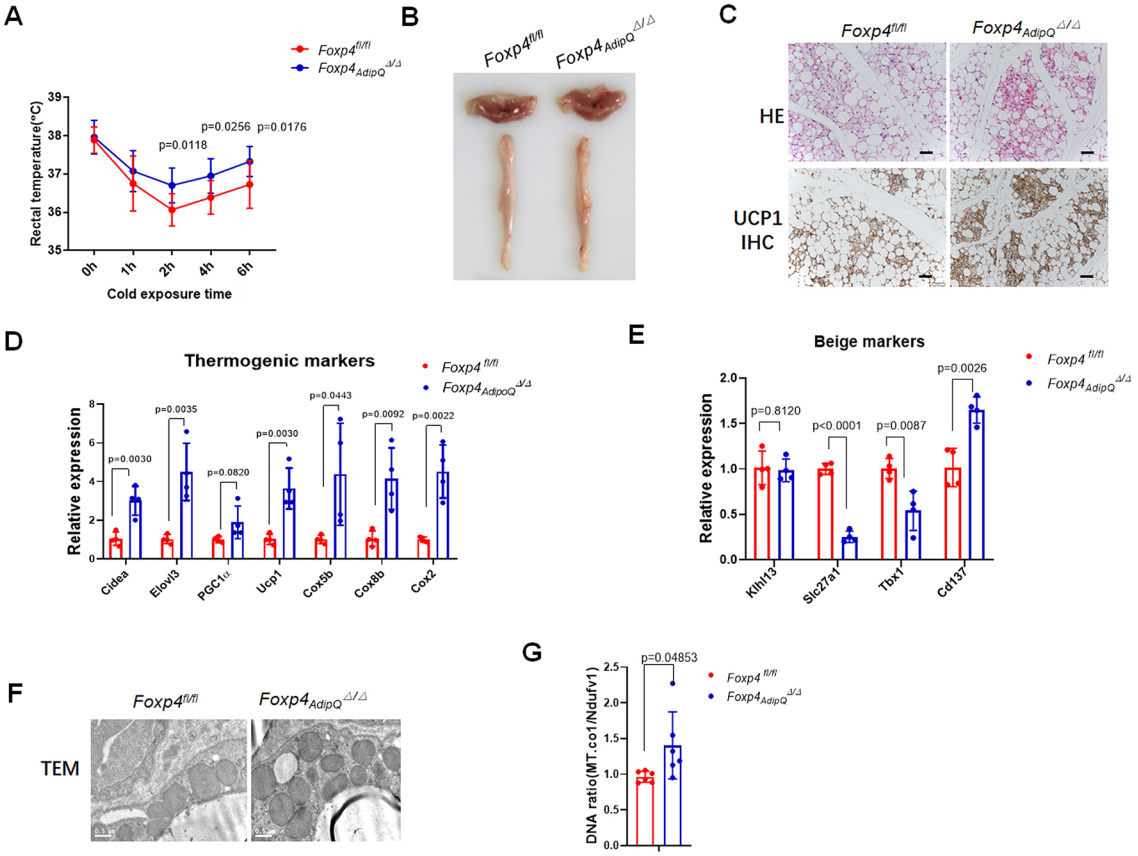

Fig. 6. Loss of *Foxp4* exacerbates beige adipocytes thermogenesis upon cold exposure. (A) Rectal temperatures of 2-month-old $Foxp4_{AdipQ}^{\Delta/\Delta}$ mice during a 6-h 4°C cold challenge. *n*=8. (B) Fat depot of BAT and sWAT in $Foxp4_{AdipQ}^{\Delta/\Delta}$ mice after 1 week of 4°C exposure. (C) HE and IHC staining for UCP1 on sWAT sections from the mice shown in B. Scale bars: 100 µm. Three independent experiments were replicated. (D,E) mRNA levels of a set of thermogenic and beige selective genes. *n*=4. (F) TEM of sWAT from the mice shown in B. Scale bars: 2 µm. Three independent experiments were replicated. (G) Mitochondria DNA abundance in sWAT of the mice shown in B. *n*=4.

Development (2022) 149, dev200260. doi:10.1242/dev.200260

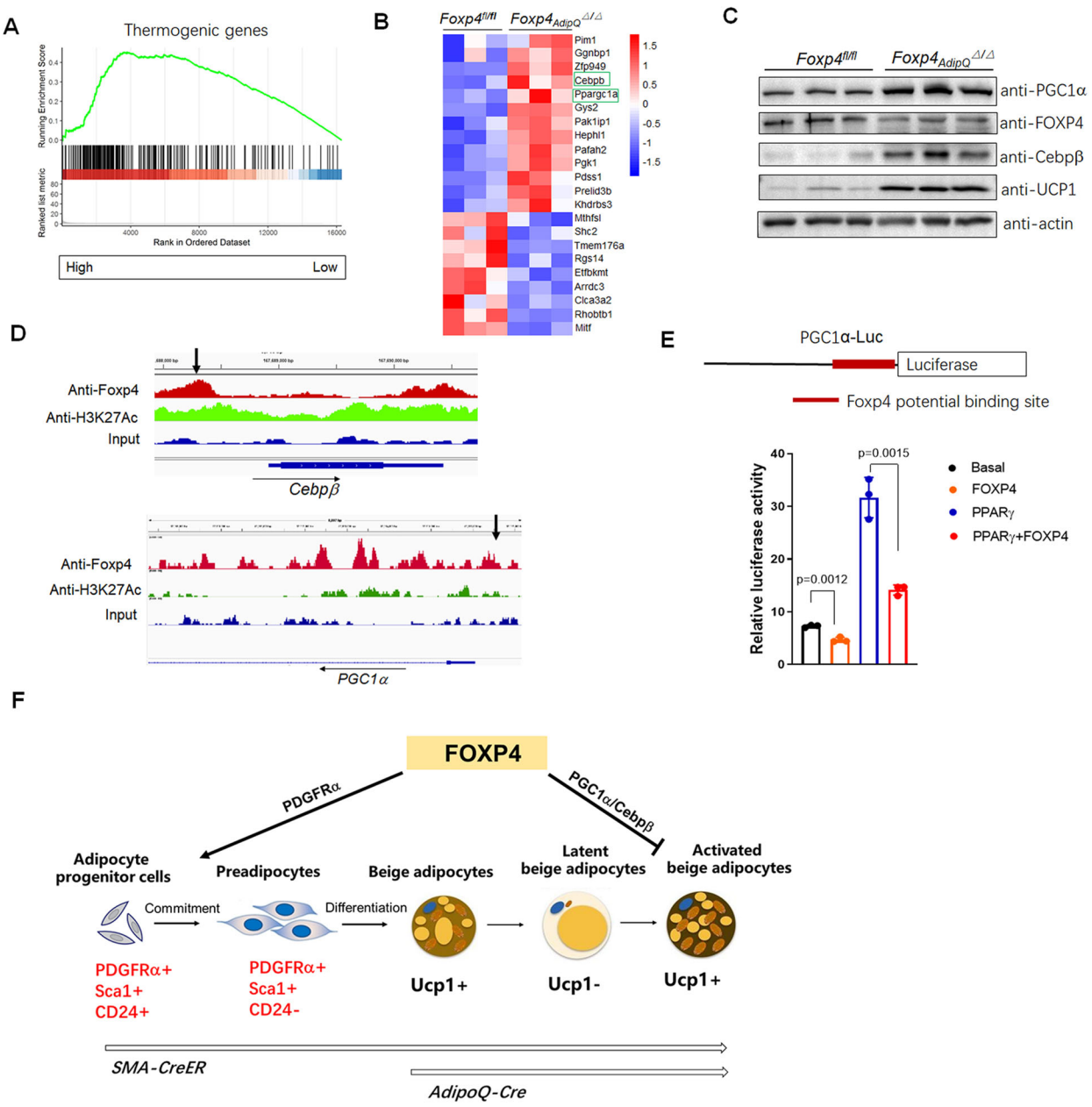

Fig. 7. FOXP4 directly regulates the expression of *Cebpb* and *Pgc1a* during beige adipocyte thermogenic activation. (A) RNA-seq analysis of thermogenic marker gene expression in sWAT of *Foxp4*$_{AdipQ}^{\Delta/\Delta}$ mice after a 1-week 4°C challenge. Three individual samples were collected for each group. (B) Heatmap of the 22 putative FOXP4-targeted gene expressions from the experiment shown in A. Chromatin occupancy analysis of ChIP-seq was conducted for SVF-derived beige adipocytes with an anti-Foxp4 antibody and 22 common targets were detected to overlap with RNA-seq results. (C) Western blot analysis showing the increase of protein expression of PGC1α, Cebpβ and UCP1 in sWAT of *Foxp4*$_{AdipQ}^{\Delta/\Delta}$ mice. Three independent experiments were replicated. (D) ChIP-seq profile showing the FOXP4-binding sites (black arrows) within *Cebpb* and *Pgc1a* promoter regions, which are consistent with the anti-H3K27Ac binding domain. (E) Luciferase reporter assay showing that FOXP4 represses the transactivation of *Pgc1a*-Luc by PPARγ protein in 3T3-L1 cell lines. The diagram above depicts the *Pgc1a*-Luc construct and potential FOXP4-binding site. Three independent experiments were replicated. (F) Schematic depicting the distinct role of FOXP4 in beige adipocyte differentiation and thermogenic activation. FOXP4 regulates beige differentiation from progenitor cells by modulating PDGFRAα signaling, whereas it arrests their activation by repressing the expression of the thermogenic genes *Pgc1a* and *Cebpb*.

plastic morphology that is tightly coupled with their reversible thermogenic potency. In this study, we dissected the phase-specific role of transcription factor FOXP4 in beige fat cell differentiation and thermogenesis. *Foxp4* deletion impaired the early differentiation of beige adipocytes from progenitor cells, but exacerbated cold-induced thermogenesis in latent beige adipocytes. Our findings indicate that FOXP4 primes beige cell differentiation, but acts as a 'brake' for beige adipocyte thermogenesis under cold challenge (Fig. 7F).

To evaluate the impact of FOXP4 on beige cell differentiation, two independent knockout models were employed in our study. In our first model, we employed *pMSCV-Cre* to delete *Foxp4* in all adipocyte precursor cells. Loss of *Foxp4* led to defective beige adipogenesis, but not brown or white adipogenesis, during

Development (2022) 149, dev200260. doi:10.1242/dev.200260

differentiation from progenitor cells. At the adult stage, the majority of cold-induced beige adipocytes arise from mural progenitor cells within vascular compartments of WAT (Long et al., 2014; Shamsi et al., 2021). As our second model, TM-inducible, Cre-mediated recombination was used to delete *Foxp4* in SMA$^+$ SVF cells prior to beige adipocyte differentiation. FACS analyses *in vivo* and *in vitro* for *Foxp4*-knockout SVF cells revealed a smaller cell proportion of adipocyte progenitor cells in the knockout mice compared with wild-type controls. Of note, the *in vivo* knockout of *Foxp4* by TM injections in *SMA-Cre^{ERT}* mice did not exhibit an obvious deficiency in beige adipocyte biogenesis, unlike *in vitro* knockout in SVF cultures by 4-OH TM or by pMSCV-Cre. In addition, expression levels of general adipogenesis markers (*Cebpa/b/g*, *Fabp4*, *Ppparg*) were not evidently altered in SMA$^+$ beige cells with *Foxp4* deficiency (Fig. S2C,D). This may be due to the targeting efficacy by *SMA-Cre^{ERT}*. It was previously shown that *SMA-Cre^{ERT}* labeling could account for ∼60% of cold-induced beige adipocytes (Berry et al., 2016). Taken together, these experiments demonstrated that FOXP4 was required for early adipocyte differentiation, especially for beige cell biogenesis.

PDGFRα-positive progenitor cells within sWAT harbor multiple potency in cell differentiation. They are precursor cells for both white and beige adipocytes (Gao et al., 2018), as well as for fibroblasts (Cattaneo et al., 2020). PDGFRα-positive progenitors give rise to beige adipocytes in response to β3-adrenoceptor activation and high-fat diet (Lee et al., 2012), rather than to cold induction (Berry et al., 2016; Shin et al., 2020). In addition, PDGFRα expression levels seem to be precisely controlled during adipogenesis. PDGFRα expression precedes beige adipocyte differentiation (Gao et al., 2018). Its continuous expression or activation in sequential phases drive progenitor cells towards a fibroblastic cell fate (Iwayama et al., 2015; Marcelin et al., 2017; Sun et al., 2017). In line with those findings, *Foxp4*-deficient SVF cells display fibroblast signatures, as well as increased *Pdgfra* expression. When combined with our ChIP-seq and luciferase reporter data, the evidence suggests that FOXP4 primes beige adipocyte differentiation, partially by modulating *Pdgfra* expression levels. Of note, we cannot exclude the possibility that the higher *Pdgfra* expression may be partially due to more residual PDGFRα$^+$ undifferentiated cells in cultures with *FOXP4* deletion. The observations of PDGFRα expression may be a combined output from these two pathways.

Prior to the present report, only a few beige-selective transcription factors had been characterized, including MRTFA (McDonald et al., 2015) and Tbx1 (Wu et al., 2012). FOXP4 is expressed in both BAT and sWAT of mice. However, our genetic analysis showed that deletion of *Foxp4* in adipocytes had little effect on *in vivo* BAT development and thermogenesis. Only oxygen consumption and expression of several thermogenic marker genes were slightly increased in *in vitro* cultures of SVF-derived brown adipocytes from *Foxp4*-deficient mice. Upon cold exposure and adrenoceptor agonist stimulation, we observed no significant differences *in vivo* in BAT thermogenesis. Its dynamic expression level in beige adipocytes during cell differentiation and cold exposure suggests that FOXP4 is a selective regulator of beige adipocyte development and cold-induced thermogenesis.

The thermogenic program of beige adipocytes can be activated through various pathways (Barbatelli et al., 2010; Rosenwald et al., 2013). Most beige adipocytes are activated through the β3-adrenergic signaling pathway (Lee et al., 2015). However, it has also been reported that cold-induced activation of beige adipocytes requires the β1 adrenergic receptor (Adrb1), but not the β3 adrenergic receptor (Adrb3) (Jiang et al., 2017). Recently, a glycolytic beige population was identified that could be induced by chronic cold adaptation in the absence of β-adrenergic receptor signaling (Chen et al., 2019). Excess calorie intake also can trigger the activation of CHRNA2-dependent beige adipocytes (Jun et al., 2020), which also are glycolytic and β-adrenergic signaling independent. Interestingly, *Foxp4*-inactivated beige adipocytes appeared to only react to cold exposure, not to an adrenoceptor agonist (Fig. S7C,D), and had elevated expressions of glycolytic marker genes compared with controls in response to cold exposure (Fig. S6C,D). This suggests that FOXP4 controls beige cell thermogenic activation through an adrenergic signaling-independent pathway, perhaps partially through a glycolytic pathway.

A recent report pointed out that different transcriptional machinery governs beige adipocyte development and activation between peri-weaning and adult stages (Wu et al., 2020). However, we observed that inactivation of *Foxp4* only slightly exacerbated UCP1-mediated thermogenesis at both stages. Thus, we suggest that FOXP4 is shared as a regulator of arresting thermogenesis in both juvenile and mature beige adipocytes. This view is consistent with previous studies from our laboratory that showed that FOXP1, a highly conserved paralog of FOXP4, repressed both beige adipocyte differentiation and UCP1-mediated thermogenesis (Liu et al., 2019). Given that FOXP1 and FOXP4 form dimers in various tissues (Li et al., 2012, 2004; Sin et al., 2015), we cannot exclude the possibility of a cooperative function of FOXP1 and FOXP4 in controlling beige cell thermogenesis.

Collectively, the data presented here reveal a role of FOXP4 in beige adipocytes differentiation and cold-induced thermogenesis. We suggest that a more thorough understanding of the underlying causes of FOXP4-selective functions will allow us to manipulate beige cells specifically to improve systemic energy metabolism and to combat obesity.

MATERIALS AND METHODS

Mice

The *Foxp4$^{fl/fl}$* constructed by our lab has been described in previous studies (Zhao et al., 2015). *Adiponectin-Cre* was obtained from The Jackson Laboratory (Stock no. 028020). *SMA-CreERT* mice was kindly provided by Prof. Gang Ma (Shanghai Jiaotong University, China). The genetic backgrounds of all knockout mice were C57Bl/6J. Mice were bred with standard rodent chow food or HFD. For cold treatment, mice were bred in a 4°C environment for a week. For continuous β-adrenergic stimulation, mice were injected intraperitoneally with CL-316,243 (0.75 mg/kg) each day for up to 7 days. Male mice were used in the experiments unless otherwise indicated. The experiments were not randomized, and the investigators were not blinded to allocation during experiments or outcome assessments. Mice are maintained under a constant environmental temperature (22°C) and a 12-h light/12-h dark cycle. All animal experiments were performed according to the ethical guidelines of Shanghai Jiao Tong University (SYXK 2011-0112).

Metabolic study

Minispec TD-NMR Analyzers (Bruker Instruments) were used to evaluate adiposity composition on anesthetized animals. Food intake, energy expenditure, O_2 consumption, CO_2 production and physical activity were measured using an indirect calorimetry system (CLAMS; Oxymax, Columbus Instruments), installed under a constant environmental temperature (22°C) and a 12-h light (07:00-19:00 h), 12-h dark cycle (19:00-07:00 h). Mice in each chamber had free access to food and water. The raw data were normalized by body weight and the histograms of day (07:00-19:00 h) and night (19:00-07:00 h) show the mean value of all points measured during the 12-h period.

Development (2022) 149, dev200260. doi:10.1242/dev.200260

Immunohistochemistry and TEM

Adipose tissues were fixed in 4% paraformaldehyde for 16 h at 4°C, embedded in paraffin or tissue freezing medium (Leica) and sectioned at 4 µm. HE staining was conducted according to standard protocols. For immunofluorescence, heat-induced antigen retrieval with sodium citrate buffer (10 mM sodium citrate, 0.05% Tween 20, pH 6.0) was performed before sections were blocked with 5% bovine serum albumin in Tris-buffered saline with 0.1% Tween 20 detergent (TBST) (pH 7.6) for 30 min at 37°C, then incubated overnight at 4°C with primary antibodies to mouse Foxp4 (Millipore, ABE74, 1:100) or UCP1 (Abcam, ab10893, 1:100). Subsequently, sections were incubated with secondary fluorescence-conjugated or horseradish peroxidase (HRP)-conjugated antibodies at 37°C for 30 min in the dark. Samples were imaged using a Leica TCS SP5 confocal microscope, Leica DM2500 microscope or Leica 3000B microscope. TEM of beige adipose tissue was carried out in accordance with a previous study (Liu et al., 2019).

Cell cultures

For SVF cell isolation, primary BAT and sWAT were digested with 1 mg ml^{-1} collagenase type I (Sigma-Aldrich) in DMEM (Invitrogen) supplemented with 1% bovine serum albumin for 25 min at 37°C, followed by filtration and density separation by centrifugation (10 min at 250 ***g***). The freshly isolated SVF cells were seeded and cultured in growth medium containing DMEM, 20% fetal bovine serum (FBS), 1% penicillin/streptomycin at 37°C with 5% CO_2 for 3 days, followed by feeding with fresh medium every 2 days to reach confluence. For brown/beige adipocyte differentiation, the cells were induced with induction medium containing DMEM, 10% FBS, 5 µg ml^{-1} insulin, 0.5 mM isobutylmethylxanthine (Sigma-Aldrich), 1 µM dexamethasone (Sigma-Aldrich), 50 nM T3 (Sigma-Aldrich) and 5 µM troglitazone (Sigma-Aldrich) for 48 h, and further in growth medium supplemented with insulin, T3 and troglitazone for 6 days, followed by 0.5 mM cyclic AMP (Sigma-Aldrich) treatment for another 4 h. For inducible knockout in beige cells, SVF from *Foxp4*$_{Sma}^{ErtΔ/Δ}$ and *Foxp4*$^{fl/fl}$ mice were expanded for 2 days with growth medium, then treated with 4-OHTM at a final concentration of 1 µM in cultures for 48 h, followed by 6-day differentiation culture without 4-OHTM. HEK293T cells (ATCC) were cultured in DMEM with 10% FBS. For Oil Red O staining, cultured cells were washed with PBS and fixed with 10% formaldehyde for 15 min at room temperature. The cells were then stained using 1 ml Oil Red O working solution (5 g/l in isopropanol) and 4 ml H_2O for 30 min. After staining, the cells were washed with 60% isopropanol and imaged.

FACS analysis

Two-month-old *Foxp4* knockout mice by *SMA-CreERT* were injected once intraperitoneally with TM dissolved in sunflower oil (Sigma-Aldrich, 100 mg/kg). After 48 h, SVF cells were isolated from mice euthanized with CO_2 according to protocols described above. Progenitor cells from SVF were expanded for 2 days in growth cultures and treated with 4-OHTM (a final concentration of 1 µM) for 24 h. Those cells were then cultured with fresh medium without TM for another 24 h before being collected for FACS analysis. 4-OHTM-administrated SVF cells were suspended in FACS buffer to a final concentration of 10^5-10^6 cells/100 µl, incubated on ice for ∼30-45 min with combinations of PerCP-CD45 (BioLegend, 103131), PerCP-CD31 (BioLegend, 102419), APC-Sca-1 (BioLegend, 122511), PE-CD140α (BioLegend, 135905), CD24-FIFC (BioLegend, 101815) antibodies. The cells then washed twice with PBS before analysis on a BD FACSCalibur. The proportion of adipocyte progenitors was analyzed with FlowJo v10 software.

Oxygen consumption assay

Primary SVF cells from BAT and sWAT were isolated and cultured for 4 days before being plated in XF cell culture microplates (Seahorse Bioscience). SVF cells (10,000 cells) were seeded in each well, and each treatment included cells from three BAT or sWAT replicates. After 6 days of differentiation, cultured adipocytes were washed twice and pre-incubated in XF medium (supplemented with 25 mM glucose, 2 mM glutamine and 1 mM pyruvate) for 1-2 h at 37°C without CO_2. The OCR was measured using an XF Extracellular Flux Analyzer (Seahorse Biosciences). Oligomycin (2 mM), FCCP (2 mM), and antimycin A (0.5 mM) were preloaded into cartridges and injected into XF wells in succession. OCR was calculated as a function of time (pmoles per minute per µg protein).

Luciferase assay

Luciferase assays were performed in HEK293T (National Collection of Authenticated Cell Cultures, SCSP-502) or 3T3-L1 (#SCSP-5038) cells. The reporter plasmid *Pgc1α-Luc*, containing a 2.6 kb fragment of the promotor region of the *Pgc1a* gene, was obtained from Dr JiQiu Wang of the Ruijin hospital (Shanghai, China). *Pdgfrα-Luc* plasmid, containing 1.3 kb of the 5′ flanking region of the *Pdgfra* gene was constructed by our lab. The primers used for amplification are shown in Table S1. The expression plasmids of *Foxp4* and *Pparg* were constructed into the pcDNA3.0 vector. Cells were transfected using FuGENE HD (Promega) in 24-well plates. The transfection amount of each plasmid was 200 ng, and the total amount of transfected DNA across each transfection was balanced by pcDNA3.0 plasmids when necessary. After 36 h, a dual luciferase assay was performed according to the manufacturer's protocols (Promega).

RNA isolation and quantitative RT-PCR

We used TRIzol (Vazyme, R401) for total RNA extraction according to the manufacturer's instructions. Extracted RNA (1 µg) was converted into cDNA using the HiScript III SuperMix for qPCR (Vazyme, R323-01). Quantitative RT-PCR (qRT-PCR) was performed using a LightCycler 480 II (Roche) and SYBR Green PCR Master Mix (Vazyme, Q711-02). Fold change was determined by comparing target gene expression with the reference gene β-actin. The primers used for qRT-PCR are shown in Table S1. For RNA-seq, total RNA extracted from sWAT with TRIzol was used for library construction and RNA sequencing (Personal Biotechnology Co., Shanghai, China).

Western blot

For western blotting, adipose tissue was homogenized and lysed with RIPA (Beyotime, P0013B). Protein samples were incubated with primary antibodies against Foxp4 (Millipore, ABE74, 1:1000), Ucp1 (Abcam, ab10893, 1:1000), Cebpβ (Santa Cruz Biotechnology, sc-150, 1:500), PGC1α (Abways, CY6630, 1:1000), β-actin (Selleck Chemicals, A1016, 1:2000) at 4°C overnight. Proteins were visualized using HRP-conjugated secondary antibody and chemiluminescent HRP substrate (Millipore).

ChIP-seq

Magna ChIP Protein A+G Magnetic Beads (20 µl; Millipore, 16-663) were washed twice with 1 ml FA buffer (10 mM HEPES, pH 7.5, 150 mM NaCl, 1 mM EDTA, 1% Triton X-100, 0.1%S sodium deoxycholate, 0.1% SDS and protease inhibitors). Beads were suspended with 1 ml FA buffer, and 4 µg antibody was added to the beads, which were then rotated for at least 2 h. Differentiated SVF cells were cross-linked using 1% formaldehyde in PBS at room temperature with rotation. Cells were then incubated with 125 mM glycine (Sangon, A610235-0500; 62.5 µl 2 M glycine/ml PBS) at room temperature for 10 min to stop cross-linking. After two washes with ice-cold PBS, cells were collected and diluted in 0.5 ml FA buffer. Cells were sonicated using a Sonics VCX130 with the following parameters: 5 s on; 10 s off; 6 min to make the DNA fragment at 300-500 bp. The sonicated solution was centrifuged at 13,000 rpm (16,200 ***g***) for 5 min and the supernatant collected. The beads bound to antibody were then washed twice with FA buffer. Antibody-coated beads were added into the sonicated supernatant for 12-16 h at 4°C with rotation. The beads were then washed with FA buffer once, then with the following buffers (twice each): high salt buffer (10 mM HEPES, pH 7.5, 150 mM NaCl, 1 mM EDTA, 1% Triton X-100, 0.1% sodium deoxycholate, 0.1% SDS); LiCl buffer (10 mM Tris-HCl, pH 8.0, 0.25 M LiCl, 1% NP-40, 1 mM EDTA, 0.1% sodium deoxycholate); TE buffer (10 mM Tris-HCl, pH 7.5, 1 mM EDTA). The beads were then suspended with 270 elution buffer (50 mM Tris-HCl, pH 7.5, 1 mM EDTA, 1% SDS) and eluted by votexing at 900 rpm for 30 min on an Eppendorf Thermo Mixer at 68°C. After elution, 130 µl TE buffer

Development (2022) 149, dev200260. doi:10.1242/dev.200260

containing 3 µl RNase A (Thermo Fisher, EN0531) was added into the eluate, and incubated at 37°C for 30 min. Then, 5 µl Proteinase K (Thermo Fisher, AM2546) was added and incubated at 65°C overnight to reverse cross-links. DNA was isolated and purified with a ZYMO DNA Clean & Concentrator (Zymo Research, D4013).

Libraries were constructed using a VAHTS Universal DNA Library Prep Kit for Illumina V3 (Vazyme, ND607) according to the manufacturer's protocol. Isolated Chip DNA was sequentially subjected to end repair/phosphorylation/A-tailing adding, and index adaptor ligation. AMPure XP beads (Beckman Coulter, A63880) were used for a post-ligation cleanup, DNA was eluted from beads and amplified by PCR for ten cycles. DNA sized between 200 and 700 bp was selected by a double-sided size selection strategy with AMPure XP beads. After elution with 10 mM Tris (pH 8.0), libraries were analyzed using the Qubit and Agilent 2100 Bioanalyzer, pooled at a final concentration of 12 pM and sequenced on a HiSeq2500. For ChIP-seq analysis, demultiplexed ChIP-seq reads were aligned to the mm10 mouse genome using Bowtie2 (Langmead and Salzberg, 2012) with the parameter '–no-discordant –no-unal –no-mixed'. PCR duplicates and low-quality reads were removed by Picard. Reads were processed using Samtools (Li et al., 2009) and subjected to peak-calling with MACS2 (Zhang et al., 2008) with a parameter 'except -f BAMPE -p 0.01'. We converted the bam file to a bw file using deeptools (v3.3.0). Integrative Genomics Viewer (IGV, v2.7.2) was used for peak visualization. Overlaps between ChIP-seq and RNA-seq were performed and Venn diagrams were drawn in R.

Glucose tolerance test

For the glucose tolerance test, mice were given an intraperitoneal injection of 100 mg/ml D-glucose (2 g/kg body weight) after overnight fasting, and tail blood glucose concentrations were measured using a glucometer (AccuCheck Active, Roche).

Data analysis

For RNA-seq analysis, sequencing reads were filtered using Cutadapt and aligned to the mm10 mouse genome using HISAT2 (Kim et al., 2015). Filtered reads were assigned to the annotated transcriptome and quantified using HTSeq (Anders et al., 2015); FPKM was used as normalization method. The analysis below was all performed in R. We used DESeq for differential expression analysis (Anders and Huber, 2010). Genes were considered significant if they passed a fold change (FC) cutoff of $|\log2FC|>0.585$ and a false discovery rate (FDR) cutoff of FDR<0.05%. Heatmap in R was used for gene expression cluster analysis and heatmap visualization. We used topGO for gene ontology analysis (Alexa et al., 2006). clusterProfiler was used for KEGG and GSEA analysis with default parameters (Yu et al., 2012).

For statistical analysis, all data are presented as mean±s.d. Two-tailed Student's *t*-tests were used for comparisons between two groups and two-way ANOVA for more than two groups.

Acknowledgements

We thank Prof. Haley O. Tucker from the University of Texas for editing the manuscript.

Competing interests

The authors declare no competing or financial interests.

Author contributions

Methodology: Z.Y., X.Z., J.W.; Software: P.L.; Validation: X.X., X.Z.; Investigation: F.W., S.X., T.C., S.L., W.Z., S.W., R.Z.; Resources: J.W.; Data curation: P.L.; Writing - original draft: X.G.

Funding

This work was supported by research grants from the National Major Fundamental Research 973 Program of China funded by the Ministry of Science and Technology of the People's Republic of China (2020YFA0803601 to X.G.) and grants from the National Natural Science Foundation of China [92068203 and 91749103 to X.G.].

Data availability

RNA-seq and ChIP-seq data have been deposited in GEO under accession numbers GSE199559, GSE199567 and GSE199570.

References

Alexa, A., Rahnenfuhrer, J. and Lengauer, T. (2006). Improved scoring of functional groups from gene expression data by decorrelating GO graph structure. *Bioinformatics* **22**, 1600-1607. doi:10.1093/bioinformatics/btl140

Altshuler-Keylin, S., Shinoda, K., Hasegawa, Y., Ikeda, K., Hong, H., Kang, Q., Yang, Y., Perera, R. M., Debnath, J. and Kajimura, S. (2016). Beige adipocyte maintenance is regulated by autophagy-induced mitochondrial clearance. *Cell Metab.* **24**, 402-419. doi:10.1016/j.cmet.2016.08.002

Anders, S. and Huber, W. (2010). Differential expression analysis for sequence count data. *Genome Biol.* **11**, R106. doi:10.1186/gb-2010-11-10-r106

Anders, S., Pyl, P. T. and Huber, W. (2015). HTSeq-a Python framework to work with high-throughput sequencing data. *Bioinformatics* **31**, 166-169. doi:10.1093/bioinformatics/btu638

Barbatelli, G., Murano, I., Madsen, L., Hao, Q., Jimenez, M., Kristiansen, K., Giacobino, J. P., De Matteis, R. and Cinti, S. (2010). The emergence of cold-induced brown adipocytes in mouse white fat depots is determined predominantly by white to brown adipocyte transdifferentiation. *Am. J. Physiol. Endocrinol. Metab.* **298**, E1244-E1253. doi:10.1152/ajpendo.00600.2009

Berry, R. and Rodeheffer, M. S. (2013). Characterization of the adipocyte cellular lineage in vivo. *Nat. Cell Biol.* **15**, 302-308. doi:10.1038/ncb2696

Berry, D. C., Jiang, Y. and Graff, J. M. (2016). Mouse strains to study cold-inducible beige progenitors and beige adipocyte formation and function. *Nat. Commun.* **7**, 10184. doi:10.1038/ncomms10184

Cattaneo, P., Mukherjee, D., Spinozzi, S., Zhang, L., Larcher, V., Stallcup, W. B., Kataoka, H., Chen, J., Dimmeler, S., Evans, S. M. et al. (2020). Parallel lineage-tracing studies establish fibroblasts as the prevailing in vivo adipocyte progenitor. *Cell Rep.* **30**, 571-582. doi:10.1016/j.celrep.2019.12.046

Chen, Y., Ikeda, K., Yoneshiro, T., Scaramozza, A., Tajima, K., Wang, Q., Kim, K., Shinoda, K., Sponton, C. H., Brown, Z. et al. (2019). Thermal stress induces glycolytic beige fat formation via a myogenic state. *Nature* **565**, 180-185. doi:10.1038/s41586-018-0801-z

Eguchi, J., Wang, X., Yu, S., Kershaw, E. E., Chiu, P. C., Dushay, J., Estall, J. L., Klein, U., Maratos-Flier, E. and Rosen, E. D. (2011). Transcriptional control of adipose lipid handling by IRF4. *Cell Metab.* **13**, 249-259. doi:10.1016/j.cmet.2011.02.005

Gao, Z., Daquinag, A. C., Su, F., Snyder, B. and Kolonin, M. G. (2018). PDGFRalpha/PDGFRbeta signaling balance modulates progenitor cell differentiation into white and beige adipocytes. *Development* **145**, dev155861.

Han, X., Zhang, Z., He, L., Zhu, H., Li, Y., Pu, W., Han, M., Zhao, H., Liu, K., Huang, X. et al. (2021). A suite of new Dre recombinase drivers markedly expands the ability to perform intersectional genetic targeting. *Cell Stem Cell* **28**, 1160-1176. doi:10.1016/j.stem.2021.01.007

Iwayama, T., Steele, C., Yao, L., Dozmorov, M. G., Karamichos, D., Wren, J. D. and Olson, L. E. (2015). PDGFRalpha signaling drives adipose tissue fibrosis by targeting progenitor cell plasticity. *Genes Dev.* **29**, 1106-1119. doi:10.1101/gad.260554.115

Jiang, Y., Berry, D. C. and Graff, J. M. (2017). Distinct cellular and molecular mechanisms for beta3 adrenergic receptor-induced beige adipocyte formation. *Elife* **6**, e30329. doi:10.7554/eLife.30329

Jun, H., Ma, Y., Chen, Y., Gong, J., Liu, S., Wang, J., Knights, A. J., Qiao, X., Emont, M. P., Xu, X. Z. S. et al. (2020). Adrenergic-independent signaling via CHRNA2 regulates beige fat activation. *Dev. Cell* **54**, 106-116. doi:10.1016/j.devcel.2020.05.017

Kim, D., Landmead, B. and Salzberg, S. L. (2015). HISAT: a fast spliced aligner with low memory requirements. *Nat. Methods* **12**, U121-U357. doi:10.1038/nmeth.3317

Langmead, B. and Salzberg, S. L. (2012). Fast gapped-read alignment with Bowtie 2. *Nat. Methods* **9**, U354-U357. doi:10.1038/nmeth.1923

Lee, Y. H., Petkova, A. P., Mottillo, E. P. and Granneman, J. G. (2012). In vivo identification of bipotential adipocyte progenitors recruited by beta3-adrenoceptor activation and high-fat feeding. *Cell Metab.* **15**, 480-491. doi:10.1016/j.cmet.2012.03.009

Lee, Y. H., Petkova, A. P., Konkar, A. A. and Granneman, J. G. (2015). Cellular origins of cold-induced brown adipocytes in adult mice. *FASEB J.* **29**, 286-299. doi:10.1096/fj.14-263038

Li, S., Weidenfeld, J. and Morrisey, E. E. (2004). Transcriptional and DNA binding activity of the Foxp1/2/4 family is modulated by heterotypic and homotypic protein interactions. *Mol. Cell. Biol.* **24**, 809-822. doi:10.1128/MCB.24.2.809-822.2004

Li, H., Handsaker, B., Wysoker, A., Fennell, T., Ruan, J., Homer, N., Marth, G., Abecasis, G., Durbin, R. and Proc, G. P. D. (2009). The Sequence Alignment/Map format and SAMtools. *Bioinformatics* **25**, 2078-2079. doi:10.1093/bioinformatics/btp352

Li, S., Wang, Y., Zhang, Y., Lu, M. M., DeMayo, F. J., Dekker, J. D., Tucker, P. W. and Morrisey, E. E. (2012). Foxp1/4 control epithelial cell fate during lung development and regeneration through regulation of anterior gradient 2. *Development* **139**, 2500-2509. doi:10.1242/dev.079699

Lidell, M. E., Betz, M. J., Dahlqvist Leinhard, O., Heglind, M., Elander, L., Slawik, M., Mussack, T., Nilsson, D., Romu, T., Nuutila, P. et al. (2013). Evidence for two types of brown adipose tissue in humans. *Nat. Med.* **19**, 631-634. doi:10.1038/nm.3017

Liu, P., Huang, S., Ling, S., Xu, S., Wang, F., Zhang, W., Zhou, R., He, L., Xia, X., Yao, Z. et al. (2019). Foxp1 controls brown/beige adipocyte differentiation and thermogenesis through regulating beta3-AR desensitization. *Nat. Commun.* **10**, 5070. doi:10.1038/s41467-019-12988-8

Long, J. Z., Svensson, K. J., Tsai, L., Zeng, X., Roh, H. C., Kong, X., Rao, R. R., Lou, J., Lokurkar, I., Baur, W. et al. (2014). A smooth muscle-like origin for beige adipocytes. *Cell Metab.* **19**, 810-820. doi:10.1016/j.cmet.2014.03.025

Ma, T. and Zhang, J. (2019). Upregulation of FOXP4 in breast cancer promotes migration and invasion through facilitating EMT. *Cancer Manag. Res.* **11**, 2783-2793. doi:10.2147/CMAR.S191641

Marcelin, G., Ferreira, A., Liu, Y., Atlan, M., Aron-Wisnewsky, J., Pelloux, V., Botbol, Y., Ambrosini, M., Fradet, M., Rouault, C. et al. (2017). A PDGFRalpha-mediated switch toward CD9(high) adipocyte progenitors controls obesity-induced adipose tissue fibrosis. *Cell Metab.* **25**, 673-685. doi:10.1016/j.cmet.2017.01.010

McDonald, M. E., Li, C., Bian, H., Smith, B. D., Layne, M. D. and Farmer, S. R. (2015). Myocardin-related transcription factor A regulates conversion of progenitors to beige adipocytes. *Cell* **160**, 105-118. doi:10.1016/j.cell.2014.12.005

Oguri, Y., Shinoda, K., Kim, H., Alba, D. L., Bolus, W. R., Wang, Q., Brown, Z., Pradhan, R. N., Tajima, K., Yoneshiro, T. et al. (2020). CD81 Controls beige fat progenitor cell growth and energy balance via FAK signaling. *Cell* **182**, 563-577. doi:10.1016/j.cell.2020.06.021

Paulo, E. and Wang, B. (2019). Towards a better understanding of beige adipocyte plasticity. *Cells* **8**, 1552. doi:10.3390/cells8121552

Roh, H. C., Tsai, L. T. Y., Shao, M., Tenen, D., Shen, Y., Kumari, M., Lyubetskaya, A., Jacobs, C., Dawes, B., Gupta, R. K. et al. (2018). Warming induces significant reprogramming of beige, but not brown, adipocyte cellular identity. *Cell Metab.* **27**, 1121-1137. doi:10.1016/j.cmet.2018.03.005

Rosenwald, M., Perdikari, A., Rulicke, T. and Wolfrum, C. (2013). Bi-directional interconversion of brite and white adipocytes. *Nat. Cell Biol.* **15**, 659-667. doi:10.1038/ncb2740

Shamsi, F., Piper, M., Ho, L. L., Huang, T. L., Gupta, A., Streets, A., Lynes, M. D. and Tseng, Y. H. (2021). Vascular smooth muscle-derived Trpv1(+) progenitors are a source of cold-induced thermogenic adipocytes. *Nat Metab* **3**, 485-495. doi:10.1038/s42255-021-00373-z

Shapira, S. N. and Seale, P. (2019). Transcriptional control of brown and beige fat development and function. *Obesity (Silver Spring)* **27**, 13-21. doi:10.1002/oby.22334

Shin, S., Pang, Y., Park, J., Liu, L., Lukas, B. E., Kim, S. H., Kim, K. W., Xu, P., Berry, D. C. and Jiang, Y. (2020). Dynamic control of adipose tissue development and adult tissue homeostasis by platelet-derived growth factor receptor alpha. *Elife* **9**, e56189. doi:10.7554/eLife.56189

Sin, C., Li, H. and Crawford, D. A. (2015). Transcriptional regulation by FOXP1, FOXP2, and FOXP4 dimerization. *J. Mol. Neurosci.* **55**, 437-448. doi:10.1007/s12031-014-0359-7

Snijders Blok, L., Vino, A., den Hoed, J., Underhill, H. R., Monteil, D., Li, H., Reynoso Santos, F. J., Chung, W. K., Amaral, M. D., Schnur, R. E. et al. (2021). Heterozygous variants that disturb the transcriptional repressor activity of FOXP4 cause a developmental disorder with speech/language delays and multiple congenital abnormalities. *Genet. Med.* **23**, 534-542. doi:10.1038/s41436-020-01016-6

Spaeth, J. M., Hunter, C. S., Bonatakis, L., Guo, M., French, C. A., Slack, I., Hara, M., Fisher, S. E., Ferrer, J., Morrisey, E. E. et al. (2015). The FOXP1, FOXP2 and FOXP4 transcription factors are required for islet alpha cell proliferation and function in mice. *Diabetologia* **58**, 1836-1844. doi:10.1007/s00125-015-3635-3

Sun, C., Berry, W. L. and Olson, L. E. (2017). PDGFRalpha controls the balance of stromal and adipogenic cells during adipose tissue organogenesis. *Development* **144**, 83-94. doi:10.1242/dev.135962

Wang, W. and Seale, P. (2016). Control of brown and beige fat development. *Nat. Rev. Mol. Cell Biol.* **17**, 691-702. doi:10.1038/nrm.2016.96

Wang, Y., Paulo, E., Wu, D., Wu, Y., Huang, W., Chawla, A. and Wang, B. (2017). Adipocyte liver kinase b1 suppresses beige adipocyte renaissance through class IIa histone deacetylase 4. *Diabetes* **66**, 2952-2963. doi:10.2337/db17-0296

Wu, J., Bostrom, P., Sparks, L. M., Ye, L., Choi, J. H., Giang, A. H., Khandekar, M., Virtanen, K. A., Nuutila, P., Schaart, G. et al. (2012). Beige adipocytes are a distinct type of thermogenic fat cell in mouse and human. *Cell* **150**, 366-376. doi:10.1016/j.cell.2012.05.016

Wu, Y., Kinnebrew, M. A., Kutyavin, V. I. and Chawla, A. (2020). Distinct signaling and transcriptional pathways regulate peri-weaning development and cold-induced recruitment of beige adipocytes. *Proc. Natl. Acad. Sci. USA* **117**, 6883-6889. doi:10.1073/pnas.1920419117

Yu, G. C., Wang, L. G., Han, Y. Y. and He, Q. Y. (2012). clusterProfiler: an R Package for comparing biological themes among gene clusters. *OMICS* **16**, 284-287. doi:10.1089/omi.2011.0118

Zhang, Y., Liu, T., Meyer, C. A., Eeckhoute, J., Johnson, D. S., Bernstein, B. E., Nussbaum, C., Myers, R. M., Brown, M., Li, W. et al. (2008). Model-based Analysis of ChIP-Seq (MACS). *Genome Biol.* **9**, R137. doi:10.1186/gb-2008-9-9-r137

Zhao, H., Zhou, W., Yao, Z., Wan, Y., Cao, J., Zhang, L., Zhao, J., Li, H., Zhou, R., Li, B. et al. (2015). Foxp1/2/4 regulate endochondral ossification as a suppresser complex. *Dev. Biol.* **398**, 242-254. doi:10.1016/j.ydbio.2014.12.007

Figure S1

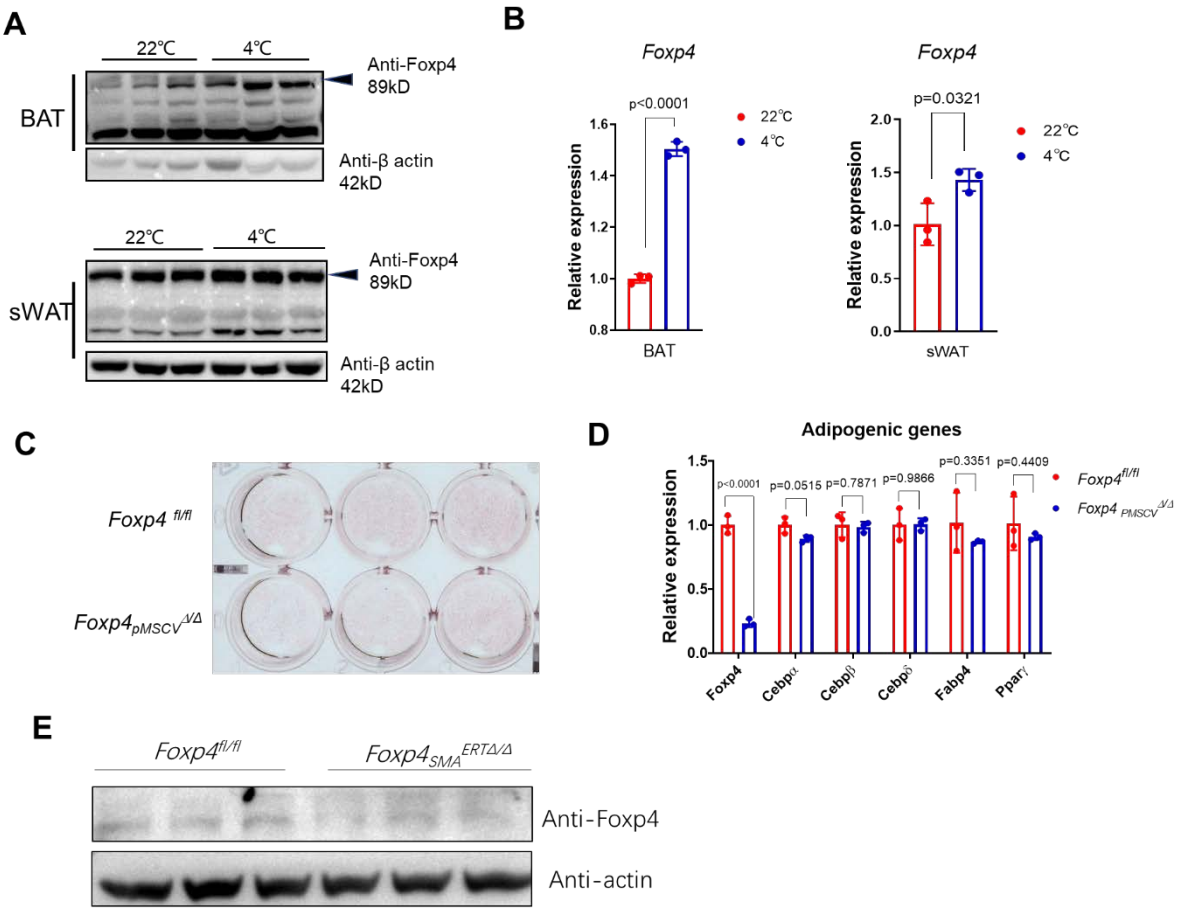

Fig. S1. Expression of *Foxp4* in adipose tissues at cold exposure, by *pMSCV-Cre* or *SMA-CreER*.

(A) Western blot for FOXP4 protein in BAT and sWAT of mice under room temperature (22℃) and one-week cold exposure (4℃). Three independent experiments were replicated.

(B) mRNA levels of *Foxp4* expression in BAT and sWAT from mice of (A). n, 3.

(C) Oil Red O staining for 8-day white adipocyte differentiation from *pMSCV-Cre*-transfected SVF of sWAT from $Foxp4^{fl/fl}$ mice.

(D) mRNA levels of adipogeniesis markers in cells of (C). n, 3.

(E) FOXP4 protein expression in SVF cells from $Foxp4_{Sma}^{ErtΔ/Δ}$ mice. Three independent experiments were replicated.

Figure S2

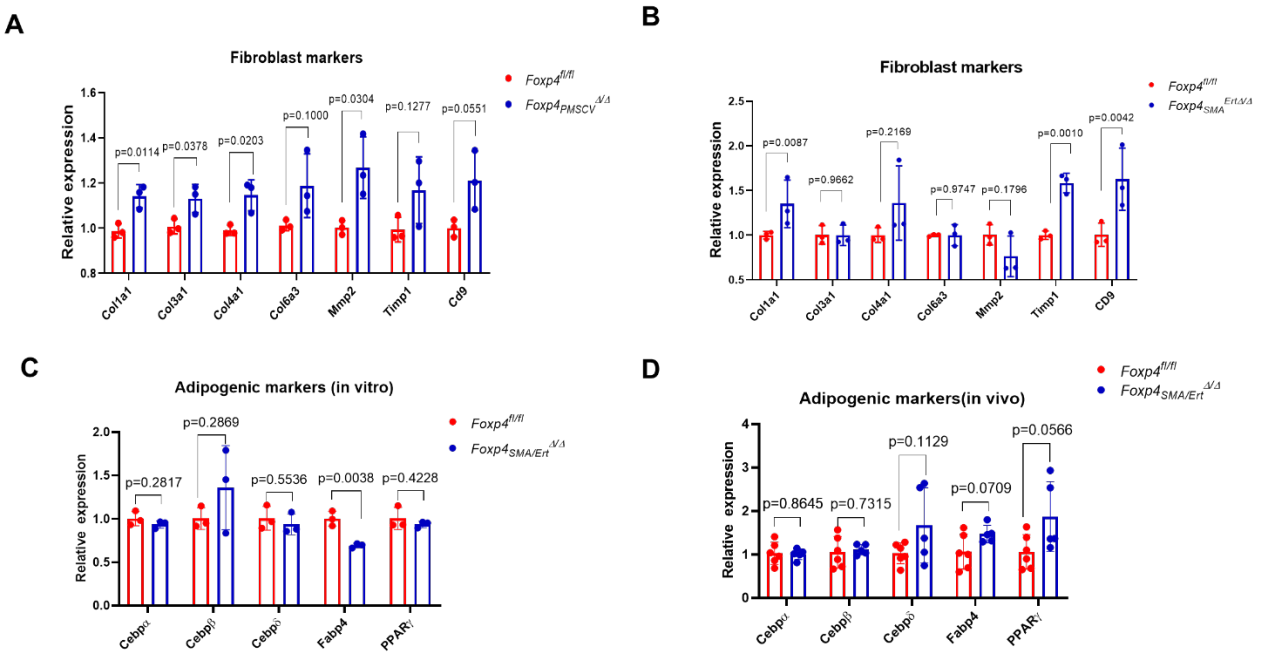

Fig. S2. *In vitro* beige adipocyte differentiation with *Foxp4* deficiency by *pMSCV-Cre*.

(A) mRNA levels of fibroblast cell marker genes in beige differentiation from SVF with *Foxp4* inactivation induced by *pMSCV-Cre*.

(B) mRNA levels of fibroblast cell marker genes in beige differentiation from SVF of $Foxp4_{Sma}^{Ert\Delta/\Delta}$ mice with *Foxp4* inactivation induced by 4-OH tamoxifen in cultures.

(C) mRNA levels of general adipogenic markers in beige differentiation from SVF of $Foxp4_{Sma}^{Ert\Delta/\Delta}$ mice with *Foxp4* inactivation induced by tamoxifen injection.

(D) mRNA levels of general adipogenic markers in beige differentiation from SVF of $Foxp4_{Sma}^{Ert\Delta/\Delta}$ mice with *Foxp4* inactivation induced by 4-OH tamoxifen in cultures.

Figure S3

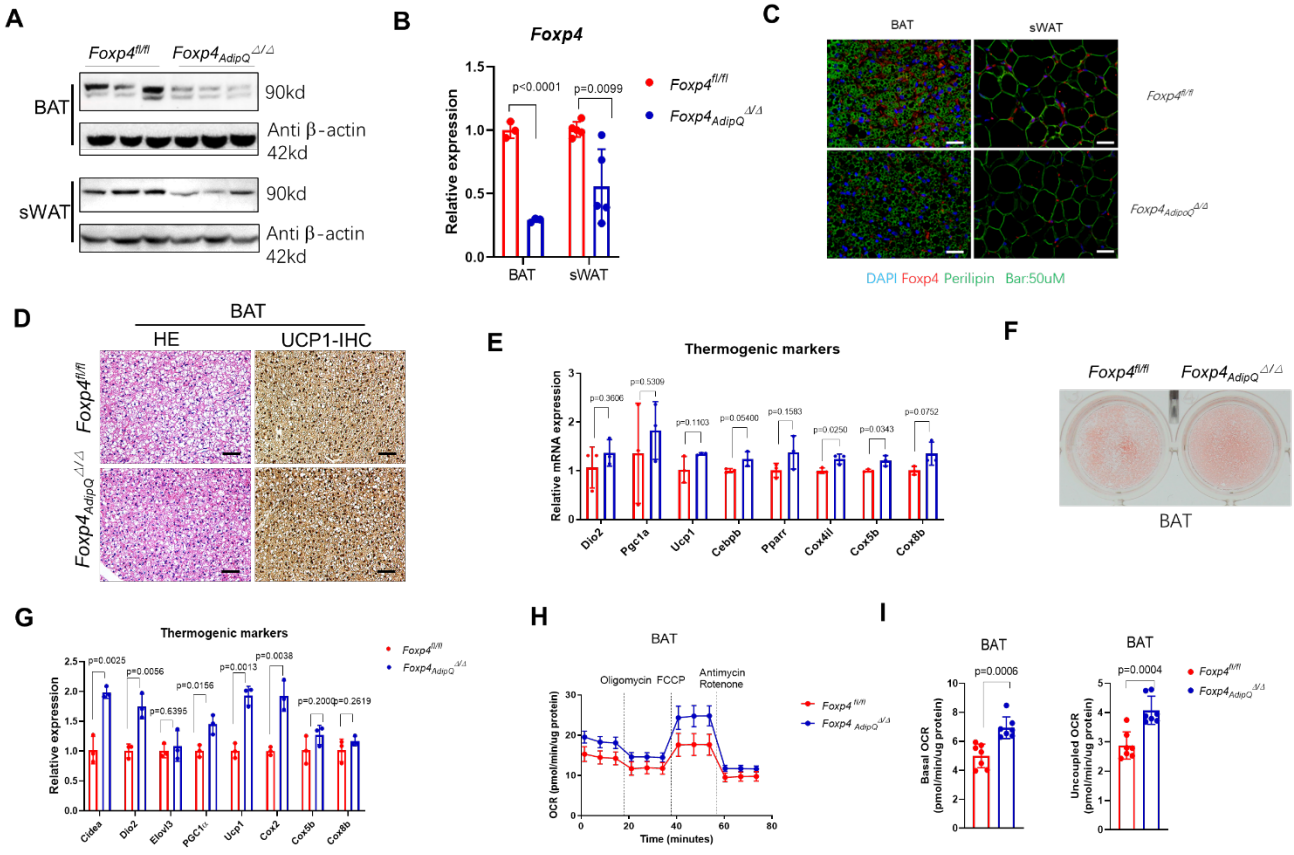

Fig. S3. Thermogenesis in BAT of *Foxp4*$_{AdipQ}^{\Delta/\Delta}$ mice.

(A) Western blot for FOXP4 protein in BAT and sWAT of *Foxp4*$^{fl/fl}$ and *Foxp4*$_{AdipQ}^{\Delta/\Delta}$ mice at age of 2 months old. Three independent experiments were replicated.

(B) Assessment of *Foxp4* mRNA expression in BAT and sWAT from mice by qPCR. n, 3~5.

(C) Immunofluorescence examination for FOXP4 on sections from BAT and sWAT of 2-month-old *Foxp4*$^{fl/fl}$ and *Foxp4*$_{AdipQ}^{\Delta/\Delta}$ mice.

(D) H&E and immunohistochemical staining (IHC) for UCP1 on BAT sections from *Foxp4*$_{AdipQ}^{\Delta/\Delta}$ mice. Three independent experiments were replicated.

(E) mRNA levels of thermogenic and mitochondrial markers in BAT.

(F) Oil Red O staining 8 day post brown adipocyte differentiation from BAT-SVF of *Foxp4*$^{fl/fl}$ and *Foxp4*$_{AdipQ}^{\Delta/\Delta}$ mice at age of 8 weeks. Three independent experiments were replicated.

(G) mRNA levels of thermogenic markers for brown adipocytes in (F). n, 3.

(H) Oxygen consumption rate (OCR) was measured for brown adipocytes from (F).

Uncoupled respiration was recorded after oligomycin inhibition of ATP synthesis, and maximal respiration following stimulation with carbonyl cyanide 4-(trifluoromethoxy) phenylhydrazone (FCCP). n,7.

(I) Quantitative analysis of basal and uncoupled OCR in (H). n, 7.

Figure S4

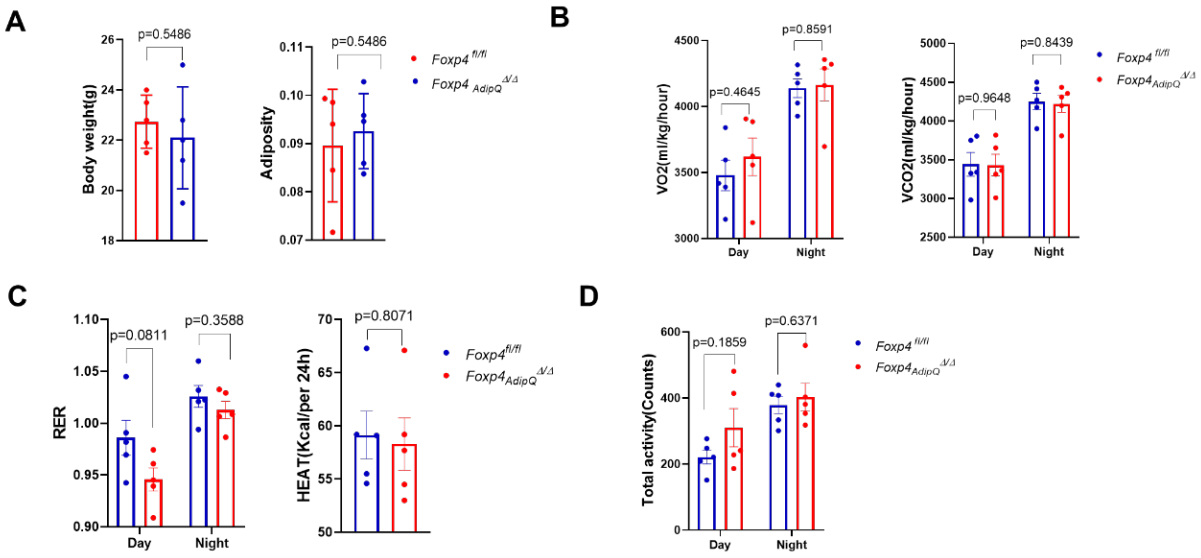

Fig. S4. Metabolic analysis for *Foxp4*$_{AdipQ}^{\Delta/\Delta}$ mice.

(A) Body weight and relative adiposity of *Foxp4*$^{fl/fl}$ and *Foxp4*$_{AdipQ}^{\Delta/\Delta}$ mice during day and night in metabolic cages at age of 3 months old. n, 5.

(B) Quantification of O_2 and CO_2 consumption of mice under room temperature. n, 5.

(C) RER and heat production of mice. n, 5.

(D) Total activity of mice. n, 5.

Figure S5

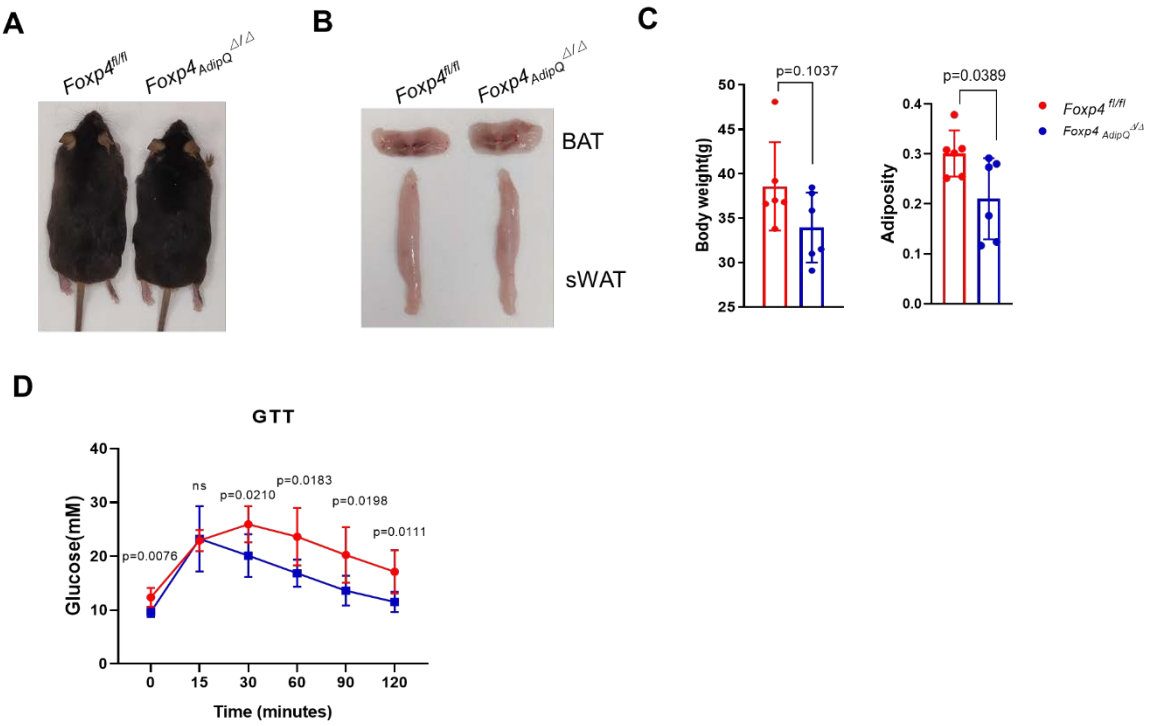

Fig. S5. *Foxp4* deficiency protects mice from HFD-fed obesity.

(A) Dorsal view of representative *Foxp4*$^{fl/fl}$ and *Foxp4*$_{AdipQ}^{\Delta/\Delta}$ mice of after 8-week feeding with HFD at age of 2 months.

(B) Representative fat depot of BAT and sWAT from mice of (A).

(C) Body weight and relative adiposity of HFD-fed mice of (A). n, 6.

(D) GTT of HFD-fed mice. n, 6.

Figure S6

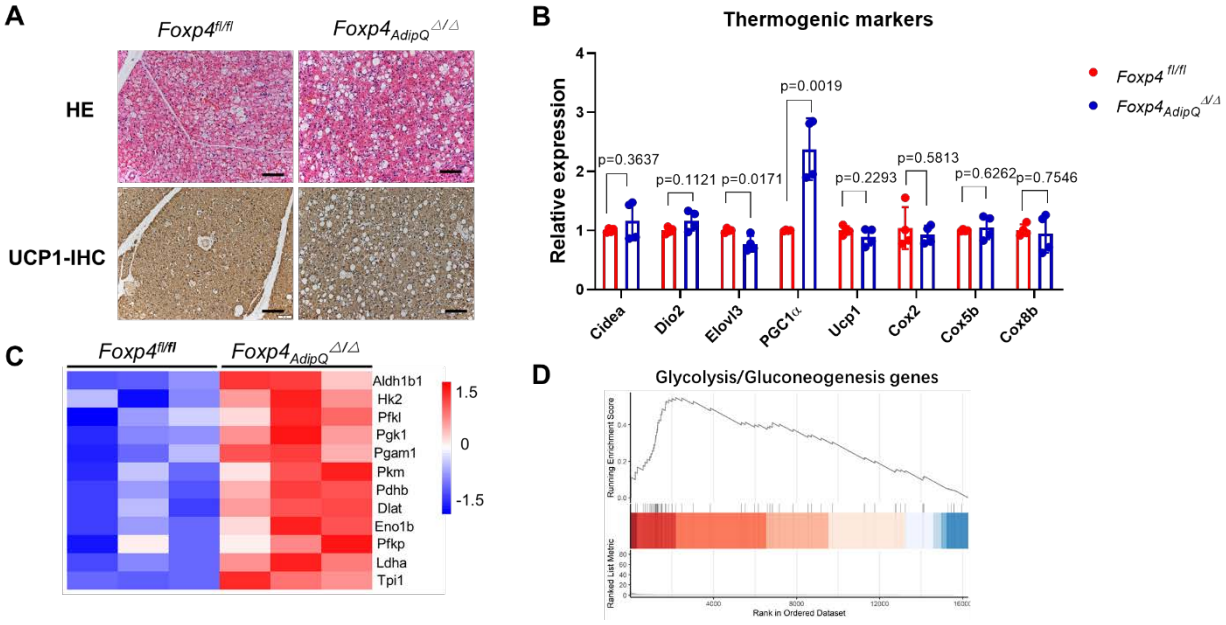

Fig. S6. BAT thermogenesis in *Foxp4*$_{AdipQ}^{\Delta/\Delta}$ mice upon cold exposure.

(A) H&E and immunohistochemistry (IHC) staining for UCP1 protein on BAT sections from *Foxp4*$_{AdipQ}^{\Delta/\Delta}$ mice after one-week cold exposure at 4℃. Three independent experiments were replicated.

(B) Thermogenesis in BAT of (A) assessed by qPCR with selective markers (*Cidea*, *Dio2*, *Elovl3*, *PGC1α*, *Ucp1*, *Cox2*, *Cox5b*, *Cox8b*). n, 3.

(C) Heatmap depicting the mRNA levels of glycolytic genes in beige adipocytes from sWAT in *Foxp4*$_{AdipQ}^{\Delta/\Delta}$ mice after one-week cold exposure at 4℃.

(D) Gene set enrichment analysis of glycolytic marker gene expressions in sWAT of (C).

Figure S7

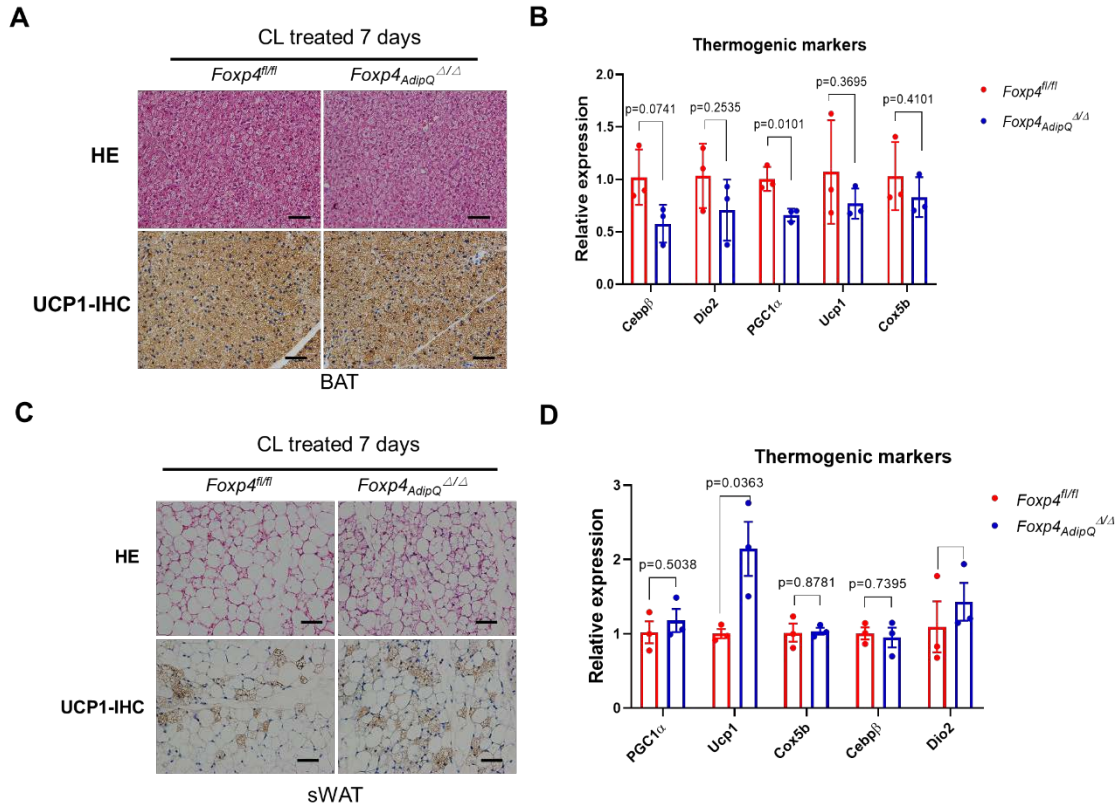

Fig. S7. Thermogenic activation in CL-316,243-stimulated *Foxp4*$^{AdipQ\Delta/\Delta}$ mice.

(A, C) H&E and IHC staining for UCP1 on BAT (A) and sWAT (C) sections from mice stimulated with CL-316,243 for 7 days. Three independent experiments were replicated.

(B, D) qPCR analysis for thermogenic gene expressions in BAT (B) and sWAT (D) from CL-316,243-stimulated mice. n, 3.

Figure S8

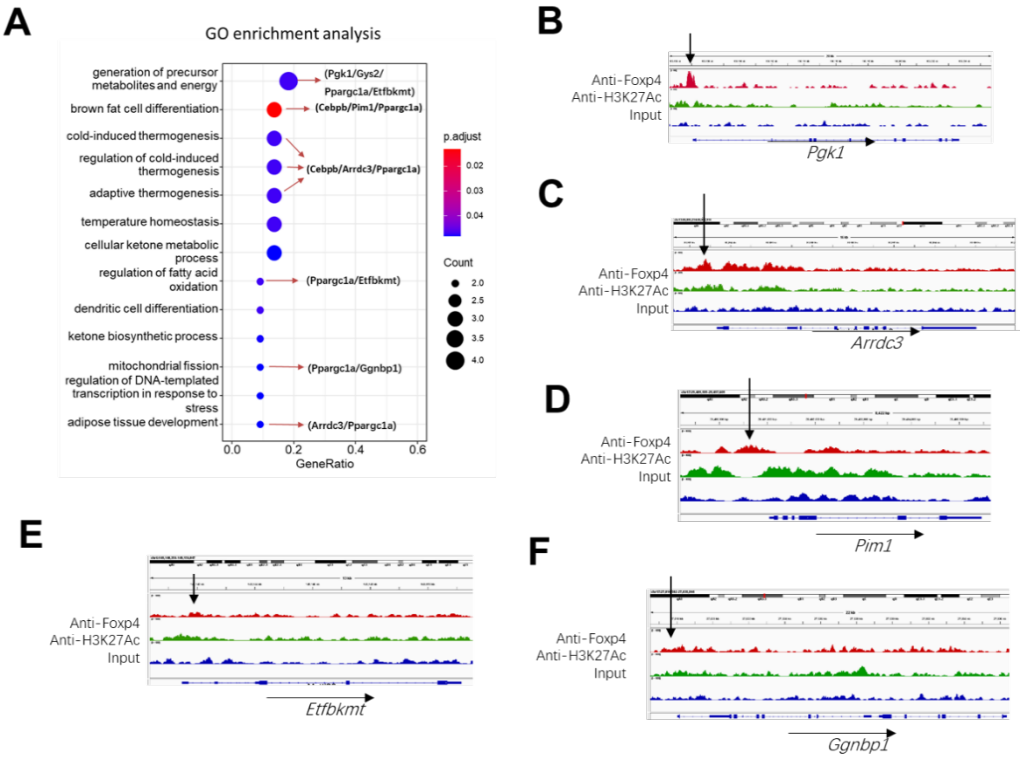

Fig. S8. Crossover examinations of RNA-seq and ChIP-seq data to identify putative FOXP4 targeting genes.

(A) GO enrichment analysis for several putative FOXP4-targeting genes.

(B-F) ChIP-seq profile showed the FOXP4 binding sites (black arrows) within *Pgk1*, *Arrdc3*, *Pim1*, *Etfbkmt*, *Ggnbp1* gene regions.

Table S1. Primers for qPCR and genotyping

primer for qPCR		
Foxp4	F	GTGTCTGTGGCCATGATGTC
	R	TCTTTGGGCTGCTGTTTTCC
Adrb3	F	GGCCCTCTCTAGTTCCCAG
	R	TAGCCATCAAACCTGTTGAGC
Ucp1	F	ACTGCCACACCTCCAGTCATT
	R	CTTTGCCTCACTCAGGATTGG
PGC1α	F	AGCCGTGACCACTGACAACGAG
	R	GCTGCATGGTTCTGAGTGCTAAG
Cebpα	F	TGGACAAGAACAGCAACGAG
	R	TCACTGGTCAACTCCAGCAC
Cebpβ	F	ACGACTTCCTCTCCGACCTCT
	R	CGAGGCTCACGTAACCGTAGT
Dio2	F	CAGTGTGGTGCACGTCTCCAATC
	R	TGAACCAAAGTTGACCACCAG
Prdm16	F	CCACCAGCGAGGACTTCAC
	R	GGAGGACTCTCGTAGCTCGAA
Cox2	F	GCAAGCATAAGACTGGACCAAA
	R	TTGTTGGCATCTGTGTAAGAGAATC
Cox4il	F	ACCAAGCGAATGCTGGACAT
	R	GGCGGAGAAGCCCTGAA
β-actin	F	AGAGGGAAATCGTGCGTGACA
	R	CACTGTGTTGGCATAGAGGTC
Elovl3	F	TCCGCGTTCTCATGTAGGTCT
	R	GGACCTGATGCAACCCTATGA
Cox5b	F	GCTGCATCTGTGAAGAGGACAAC
	R	CAGCTTGTAATGGGTTCCACAGT
Cox8b	F	TGTGGGGATCTCAGCCATAGT
	R	AGTGGGCTAAGACCCATCCTG
PPARα	F	GCGTACGGCAATGGCTTTAT
	R	GAACGGCTTCCTCAGGTTCTT
PPARγ	F	GGAAAGACAACGGACAAATCAC
	R	TACGGATCGAAACTGGCAC
Cox7a1	F	CAGCGTCATGGTCAGTCTGT
	R	AGAAAACCGTGTGGCAGAGA
Cidea	F	TGCTCTTCTGTATCGCCCAGT
	R	GCCGTGTTAAGGAATCTGCTG

Rgs2	F	GAGAAAATGAAGCGGACACTCT
	R	GCAGCCAGCCCATATTTACTG
CD137	F	CGTGCAGAACTCCTGTGATAAC
	R	GTCCACCTATGCTGGAGAAGG
Them26	F	ACCCTGTCATCCCACAGAG
	R	TGTTTGGTGGAGTCCTAAGGTC
Tbx1	F	GGCAGGCAGACGAATGTTC
	R	TTGTCATCTACGGGCACAAAG
Cd40	F	TTGTTGACAGCGGTCCATCTA
	R	CCATCGTGGAGGTACTGTTTG
Ear2	F	CCTGTAACCCCAGAACTCCA
	R	CAGATGAGCAAAGGTGCAAA
Klhl13	F	AGAATTGGTTGCTGCAATACTCC
	R	AAGGCACAGTTTCAAGTGCTG
Slc27a1	F	CTGGGACTTCCGTGGACCT
	R	TCTTGCAGACGATACGCAGAA
primer for genotyping		
Foxp4-Floxed	F	TGGAGGGACTGGGATTAGAAC
	R	ACGGGAGGCTGAACAACAC
Cre	F	TTTCCCGCAGAACCTGAAGA
	R	GGTGCTAACCAGCGTTTTCGT
***Pdgfrα*-Luc**		
Pdgfrα-promoter	F	CAGAGGGCAGGCATTTGGTAGT
	R	GCTTACTGGGACGAACACCA